cmgh
CELLULAR AND MOLECULAR GASTROENTEROLOGY AND HEPATOLOGY

ORIGINAL RESEARCH

# Acute Intestinal Inflammation Depletes/Recruits Histamine-Expressing Myeloid Cells From the Bone Marrow Leading to Exhaustion of MB-HSCs

Na Fu,[1,2,3,*] Feijing Wu,[1,2,4,*] Zhengyu Jiang,[1,2] Woosook Kim,[1,2] Tuo Ruan,[1,2,5] Ermanno Malagola,[1,2] Yosuke Ochiai,[1,2] Osmel Companioni Nápoles,[1,2] Giovanni Valenti,[1,2] Ruth A. White,[1,2] Bryana R. Belin,[1,2] Leah B. Zamechek,[1,2] Jonathan S. LaBella,[1,2] and Timothy C. Wang[1,2]

[1]*Division of Digestive and Liver Diseases, Department of Medicine, Columbia University, College of Physicians and Surgeons, New York, New York;* [2]*Herbert Irving Comprehensive Cancer Center, Columbia University Medical Center, New York, New York;* [3]*Department of Traditional and Western Medical Hepatology, Third Hospital of Hebei Medical University, Shijiazhuang, Hebei, China;* [4]*The Second Affiliated Hospital of Fujian Medical University, Quanzhou, Fujian, China;* [5]*Union Hospital, Tongji Medical College, Huazhong University of Science and Technology, Wuhan, Hubei, China*

## SUMMARY

This work highlights the interaction between bone marrow and colon in the context of acute myeloid demand and stem cell depletion, and proposes a promising therapeutic approach to address the situation in which detrimental disorders are caused by acute myeloid-biased hematopoietic stem cell exhaustion.

**BACKGROUND & AIMS:** Histidine decarboxylase (HDC), the histamine-synthesizing enzyme, is expressed in a subset of myeloid cells but also marks quiescent myeloid-biased hematopoietic stem cells (MB-HSCs) that are activated upon myeloid demand injury. However, the role of MB-HSCs in dextran sulfate sodium (DSS)-induced acute colitis has not been addressed.

**METHODS:** We investigated HDC+ MB-HSCs and myeloid cells by flow cytometry in acute intestinal inflammation by treating HDC–green fluorescent protein (GFP) male mice with 5% DSS at various time points. HDC+ myeloid cells in the colon also were analyzed by flow cytometry and immunofluorescence staining. Knockout of the HDC gene by using HDC-/-; HDC-GFP and ablation of HDC+ myeloid cells by using HDC-GFP; HDC–tamoxifen-inducible recombinase Cre system; diphtheria toxin receptor (DTR) mice was performed. The role of H2-receptor signaling in acute colitis was addressed by treatment of DSS-treated mice with the H2 agonist dimaprit dihydrochloride. Kaplan–Meier survival analysis was performed to assess the effect on survival.

**RESULTS:** In acute colitis, rapid activation and expansion of MB-HSC from bone marrow was evident early on, followed by a gradual depletion, resulting in profound HSC exhaustion, accompanied by infiltration of the colon by increased HDC+ myeloid cells. Knockout of the HDC gene and ablation of HDC+ myeloid cells enhance the early depletion of HDC+ MB-HSC, and treatment with H2-receptor agonist ameliorates the depletion of MB-HSCs and resulted in significantly increased survival of HDC-GFP mice with acute colitis.

**CONCLUSIONS:** Exhaustion of bone marrow MB-HSCs contributes to the progression of DSS-induced acute colitis, and preservation of quiescence of MB-HSCs by the H2-receptor agonist significantly enhances survival, suggesting the potential for therapeutic utility. *(Cell Mol Gastroenterol Hepatol 2021;11:1119–1138; https://doi.org/10.1016/j.jcmgh.2020.11.007)*

*Keywords:* Histidine Decarboxylase (HDC); Hematopoietic Stem Cell (HSC); Myeloid Cell; Intestine Inflammation; H2-Receptor (H2R) Agonist.

Bone marrow–derived myeloid cells are thought to play key roles in the response to intestinal injury. With severe injury to the intestine, barrier function is breached, leading to a rapid influx of immature myeloid cells as first responders.[1] After activation by Toll-like receptors and other signals,[2] myeloid cells defend against infection by bacteria, killing and phagocytizing microorganisms and removing cellular debris, but myeloid cells also contributed to epithelial regeneration through secretion of numerous growth factors.[3,4] Recently, their role in regulating intestinal

*Authors share co-first authorship.

***Abbreviations used in this paper:*** **ABX, antibiotics; BAC, bacterial artificial chromosome; BM, bone marrow; BrdU, bromodeoxyuridine; CreERT, tamoxifen-inducible recombinase Cre system; DSS, dextran sulfate sodium; FACS, fluorescence-activated cell sorting; GM-CSF, granulocyte-macrophage colony-stimulating factor; GFP, green fluorescent protein; HDC, histidine decarboxylase; HSC, hematopoietic stem cell; HSPC, hematopoietic stem and progenitor cells; H2R, H2-receptor; IBD, inflammatory bowel disease; iDTR, inducible diphtheria toxin receptor; IL, interleukin; LPS, lipopolysaccharide; MB-HSC, myeloid-biased hematopoietic stem cell; mRNA, messenger RNA; PBS, phosphate-buffered saline; qRT-PCR, quantitative reverse-transcription polymerase chain reaction; TLR, Toll-like receptor; WT, wild-type.**

Most current article



2352-345X
https://doi.org/10.1016/j.jcmgh.2020.11.007

progenitors in sepsis-like inflammatory states was defined.[5,6] In sepsis-like inflammatory states, mature granulocytic cells are released into the circulation, depleting the bone marrow and thereby stimulating increased production. With continued demand, the rapid efflux of bone marrow myeloid cells leads to activation of hematopoietic stem cells (HSCs), in part owing to loss of suppressive niche signals such as histamine signaling.[7] In bacterial sepsis, there is a causative link between lipopolysaccharide (LPS) signaling and the exhaustion of HSCs, defined as a progressive decrease in the number of functional HSCs secondary to enhanced cell cycling and a known cellular mechanism of bone marrow failure. Hyperproliferation of HSCs during acute infection leads to loss or depletion of quiescent long term HSCs.[8] Indeed, if large numbers of neutrophils are used up during infection, a process called *emergency granulopoiesis* replaces normal steady-state granulopoiesis to rapidly increase neutrophil formation, but at the expense of depleting LT-HSCs.[9] HSC exhaustion has been linked to poor outcomes in gastrointestinal-associated sepsis, but the mechanisms have not been well defined.

Acutely, severe gut injury can overwhelm the host and lead to septic shock, cytokine storm, HSC exhaustion, and organ failure. Although mature myeloid cells are recognized to home to the gut in acute inflammatory states to fight infection and promote intestinal repair, less is known regarding the HSCs that produce these regenerative blood cells and their regulation in acute intestinal inflammation. All leukocytes, including both myeloid and lymphoid cells, are derived from HSCs. However, although HSCs were for years considered as a homogeneous population, they are now recognized to display heterogeneity and comprise discrete lineages.[10] Growing evidence supports the presence of a myeloid-biased HSC (MB-HSC) that is distinct from the lymphoid-biased HSC.[11,12] In addition, quiescent HSCs become activated primarily under conditions of injury or distress.[13] Indeed, in a previous study, we showed that in models of LPS-induced sepsis or irradiation, the subset of HSCs marked by expression of histidine decarboxylase (HDC) became activated and then exhausted.[14]

Histamine is a biogenic amine that has well-defined roles in allergic responses, gastric acid secretion, and immune responses,[15–17] particularly in myeloid cells.[16–18] Endogenous histamine is generated through conversion of L-histidine to histamine by the action of a unique enzyme, HDC. The enzyme HDC now is recognized to play a key role in the regulation of inflammation and myeloid cells, and in an earlier study we discovered that HDC is expressed at low levels in MB-HSCs. We also found that HDC is expressed in the vast majority (approximately 90%) of CD11b+Gr1+ immature myeloid cells, where it regulates their maturation and production from MB-HSCs through the H2 receptor (H2R). HDC-/- mice show much more active MB-HSCs, and thus greater circulating levels of immature myeloid cells, with reduced maturation of macrophages and neutrophils.[1] Indeed, HDC marks a specific myeloid lineage that includes the quiescent MB-HSCs, which are activated during myeloid demand injury,[10] giving rise to the subset of TLR-expressing leukocytes primarily involved in inflammatory and regenerative conditions of the gut. Studies to date have indicated that HDC+ HSCs represent a more myeloid-specific subset within the clusters of differentiation (CD) 150 high expression cells HSC pool, and one that can be defined as MB-HSC.[14]

Dimaprit, a highly specific histamine H2R agonist, is reported to play an important role in several pathologic progress. Dimaprit has been shown to inhibit nitric oxide synthase,[19] suppress cytokine release in ischemia-induced liver injury,[20] and suppress tumor necrosis factor-$\alpha$ messenger RNA (mRNA) in human peripheral blood monocytes in a dose-dependent manner.[21] Dimaprit also has antitumor activity in vivo and in vitro.[22] We previously showed that dimaprit was able to prolong the survival of mice that received irradiation by preserving the quiescent status of bone marrow (BM) MB-HSCs.[14] However, the role of dimaprit in dextran sulfate sodium (DSS)-induced acute colitis has not been studied.

In this study, we sought to explore the role of HDC-expressing myeloid cells and MB-HSC in the setting of acute colitis, using DSS-induced intestinal injury as our model, a commonly used model of inflammatory bowel disease (IBD).[23,24] We found that acute colitis rapidly recruits myeloid cells from the bone marrow to the intestine, depleting the normal BM histamine niche, leading to activation and depletion of the MB-HSC. Knockout of the HDC gene worsened this phenotype and decreased survival, whereas treatment with the H2R agonist dimaprit ameliorated both HSC loss and improved survival. Overall, the data support the important role of HDC-derived histamine in modulating the response to severe intestinal inflammation.

## Results

### Activation and Depletion of HDC+ MB-HSCs in DSS-Induced Acute Colitis

To investigate the role of MB-HSCs in response to intestinal injury, we chose to study mice treated with DSS in the drinking water, which can lead to severe colitis and even death.[25–27] HDC-green fluorescent protein (GFP) mice were treated with 5% DSS and followed up for up to 1 week (Figure 1*A*). The percentage of body weight (Figure 1*B*) was decreased on day (d)5 ($P < .01$) and d7 ($P < .01$), and the ratio of spleen weight to body weight (Figure 1*C*) was increased on d7 ($P < .01$) of DSS treatment. Histologic analysis with H&E staining showed the severity of colitis was increased from d1 to d7 after DSS treatment, the injury included mild to severe infiltration inflammatory cell and extend to submucosa or even transmural on d5 and d7 after DSS initiation (Figure 1*D*), and the histologic scores were highly increased on d3, d5, and d7 compared with controls ($P < .01$, respectively) (Figure 1*E*). In this model of acute colitis, we detected by fluorescence-activated cell sorting (FACS) analysis (Figure 1*F*) HDC-GFP+ HSCs in both the bone marrow (Figure 2*A*) and the spleen. The percentage of HDC+ HSCs in the bone marrow among lineage-negative cells ($P < .05$ on d5; $P < .01$ on d7) (Figure 2*B*) and total HDC+ HSCs ($P < .01$ on d1, d5, and d7; $P < .05$ on d3) (Figure 2*C*) was increased on d1 and decreased rapidly on d3, d5, and d7, in parallel with the progression of colitis. On

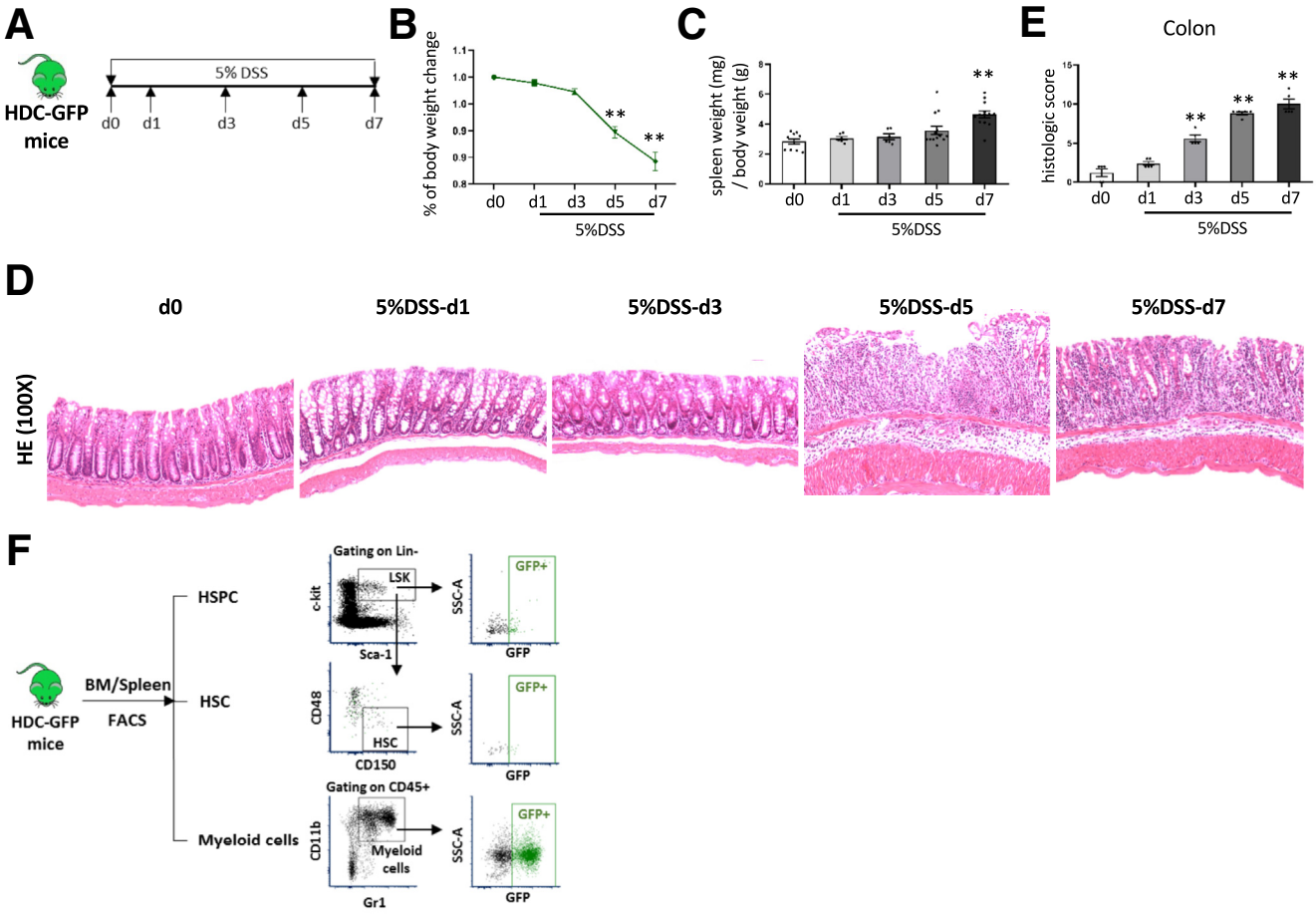


**Figure 1. DSS-induced acute colitis.** (*A*) Protocol of setting up DSS-induced acute colitis. Analysis of (*B*) body weight change and the (*C*) ratio of spleen weight (mg) to body weight (g) of HDC-GFP mice treated with DSS at different time point. (*D*) The severities of DSS-induced acute colitis were observed by H&E staining and (*E*) evaluated by histologic scores. (*F*) Strategy of FACS to analyze the HSPCs, HSCs, and myeloid cells from mouse BM and spleen. Data are expressed as means ± SEM. Results are representative of at least 3 independent experiments. $^{**}P < .01$. SSC-A, side scatter area.

d7 of the DSS colitis model, the percentage of HDC+ HSCs among lineage-negative cells decreased to almost 40% compared with normal control ($P < .05$) (Figure 2*B*), and among whole HSCs, HDC+ HSCs decreased to 25% on d7 ($P < .01$) (Figure 2*C*). In addition, the absolute number of HDC+ HSCs was decreased with the progression of colitis, especially on d5 and d7 ($P < .01$, respectively) (Figure 2*D*), and the number of HDC+ HSCs was correlated negatively with histologic scores ($P = .0001$) (Figure 2*E*). The loss in BM HDC+ HSCs presumably was related to their activation and further differentiation, which was supported by the 1.9-fold increase in the BM on d7 of myeloid-biased multipotent progenitor (MPP3), the myeloid-biased MPP ($P < .05$ on d5; $P < .01$ on d7) (Figure 2*F*).

Similar trends were evident in the spleen, as the percentage of HDC+ HSCs among lineage-negative cells ($P < .05$) (Figure 2*G*) and total HDC+ HSCs (Figure 2*H*) was increased on d3, and then decreased to 32.1% and 36.5% on d7 of severe colitis. The absolute number of HDC+ HSCs in the spleen also was increased on d3 and decreased to 55.3% on d5 ($P < .05$) (Figure 2*I*) and 39.6% on d7 ($P < .05$) (Figure 2*I*). Moreover, MPP3 was 2.1-fold increased on d7 of DSS-induced colitis ($P < .01$) (Figure 2*J*), again suggesting a sequence of activation and later differentiation by HDC+ HSCs, leading to an eventual decrease in later stages of DSS colitis.

Cell-cycle analysis of bone marrow hematopoietic stem and progenitor cells (HSPCs) showed that the BM HDC+ HSPCs, but not the HDC- HSPCs, had 19% lower ($P < .01$) and 12% lower ($P < .01$) percentages of cells in G0 after 5 days of DSS treatment (Figure 2*K* and 2*L*), and the percentage of the bromodeoxyuridine (BrdU)+ cells among HDC+ HSCs was increased from d1 to d7 ($P < .01$ respectively) (Figure 2*M*), especially a 2.3-fold and 2.6-fold increase on d5 and d7 after DSS treatment. Taken together, these data indicate that DSS-induced colonic injury propels the quiescent HDC+ HSCs out of G0, leading to the activation and proliferation of HDC+ HSPCs.

## *HDC+ Myeloid Cells Derived From BM Are Mobilized Into Circulation and Recruited to the Colon*

Histamine, made primarily by immature myeloid cells, is a key niche factor for MB-HSCs, and thus raises the question

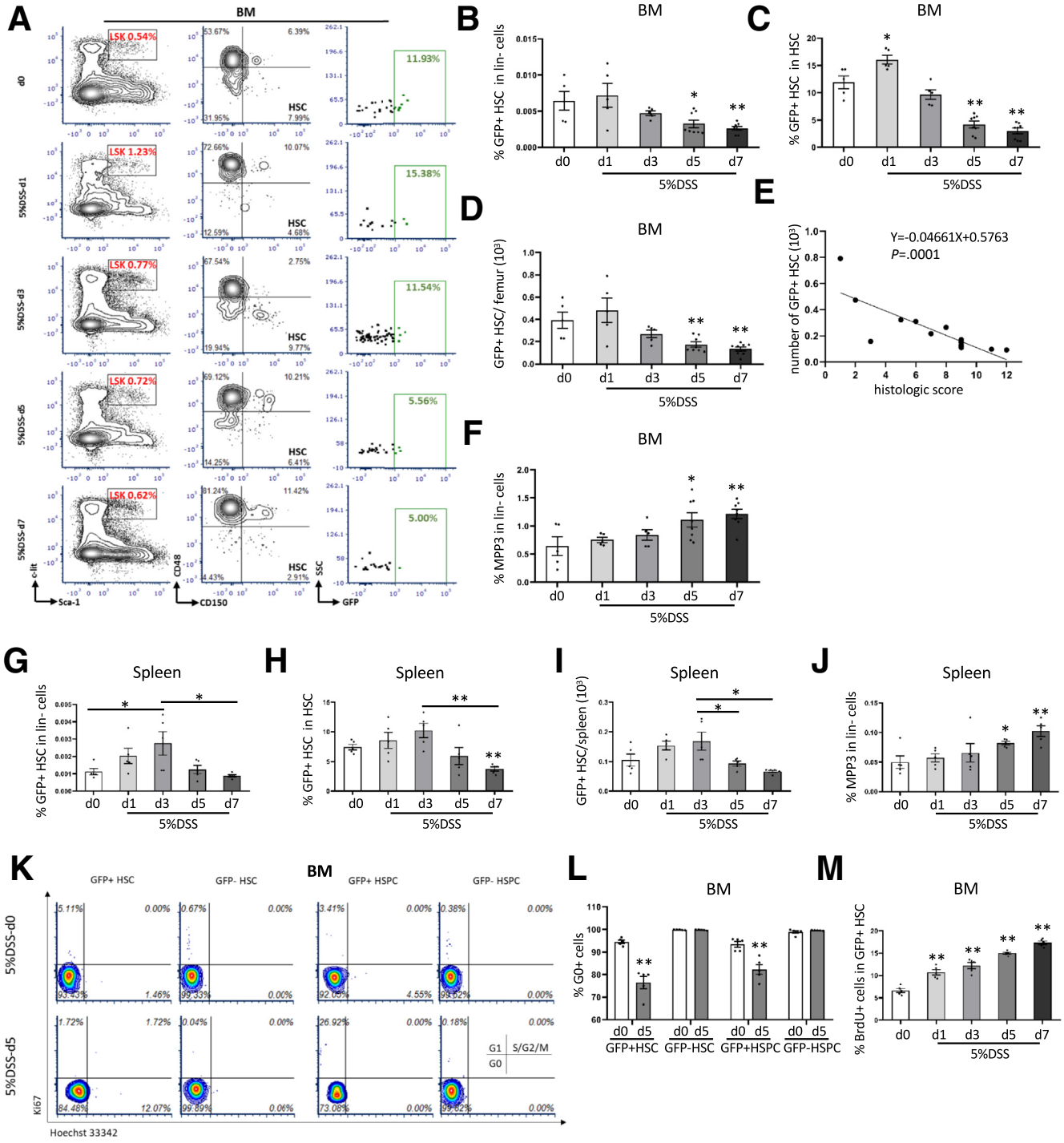


**Figure 2. BM MB-HSCs were activated and depleted in DSS-induced acute colitis.** (*A*) FACS plots showed the percentage of HSPCs (Lin−c-kit+Sca-1+, LSK), HSCs, and GFP+ HSCs among up-level populations from different time points of 5% DSS treatment. Comparison of the percentage of GFP+ HSCs among (*B*) lineage-negative cells and (*C*) HSCs from different time points of 5% DSS treatment. (*D*) Number of BM GFP+ HSCs from different time points of 5% DSS treatment. (*E*) Correlation analysis between the number of BM GFP+ HSCs and the histologic score of DSS-induced colitis. (*F*) Percentage of GFP+MPP3 among lineage-negative cells from different time points of 5% DSS treatment. Comparison of the percentage of GFP+ HSCs among (*G*) lineage-negative cells and (*H*) HSCs, and (*I*) the number of GFP+ HSCs from spleen at different time points of 5% DSS treatment. (*J*) Percentage of GFP+MPP3 among lineage-negative cells from spleen at different time points of 5% DSS treatment. Cell-cycle analysis with FACS for (*K*) Ki67 and Hoechst 33342 staining and (*L*) the percentage of G0 cells of BM HSCs and HSPCs at 5 days after 5% DSS treatment compared with the control group. (*M*) Percentage of BrdU+ cells of BM GFP+ HSCs from different time points of 5% DSS treatment. Data are expressed as means ± SEM. Results are representative of at least 3 independent experiments. *$P < .05$, **$P < .01$.

as to whether the loss of histamine could play a pivotal role in DSS-induced HSC depletion. Thus, we investigated possible changes in histamine-secreting, HDC+ myeloid cells during DSS colitis. In DSS colitis, we found that the percentages of HDC+ myeloid cells among BM CD45+ cells ($P < .01$ on d7) and the total number of HDC+ myeloid cells ($P < .05$ on d5 and d7) were decreased between d1 and d7 (Figure 3*A* and *C*). In particular, the total number of BM HDC+ myeloid cells was decreased to 63% lower on d5 and 59% lower on d7 ($P < .5$ on d5 and d7) (Figure 3*C*), which could result in a marked loss of BM histamine production. In addition, the percentage of HDC+ myeloid cells among total myeloid cells gradually increased from d1 to d7, with a 1.6-fold increase by d7 ($P < .01$) (Figure 3*B*). However, in the spleen, the percentages of HDC+ myeloid cells among CD45+ cells and the total number of HDC+ myeloid cells were increased on d5 (approximately 2.3-fold and 2.7-fold, respectively; $P < .05$) (Figure 3*D* and *F*). In addition, the percentage of HDC+ myeloid cells among total myeloid cells in the spleen was decreased significantly on d1 and increased on d7 ($P < .05$ on d1 and d7) (Figure 3*E*). Taken together, this suggests that HDC+ myeloid cells in DSS colitis are recruited primarily from the BM rather than the spleen, leading to a preferential shift toward the HDC+ myeloid lineage by BM HSCs.

Given the loss of BM myeloid cells in the setting of severe colitis, we postulated that this might impact the leukocyte population in the circulation and the colon (Figure 3*G*). Indeed, we found that the percentage of HDC+ myeloid cells among circulating CD45+ cells increased from d1 to d7 ($P < .01$) (Figure 3*H*), with an up to 3.1-fold increase on d7, with a similar increase in the percentage of HDC+ myeloid cells among total myeloid cells ($P < .01$) (Figure 3*G* and *I*). Furthermore, in the colon, we found the percentage of HDC+ myeloid cells among CD45+ cells ($P < .01$) (Figure 3*J*) and among total myeloid cells ($P < .01$) (Figure 3*G* and *K*) was increased markedly from d1 to d7 after DSS treatment. Increased infiltration in the colon by HDC+ myeloid cells also was shown through immunofluorescence imaging of frozen colon tissue from DSS-treated HDC-GFP mice (Figure 3*L* and *M*), which showed a greater density of HDC+ myeloid cells in DSS colitis ($P < .01$ at each time point).

## HDC Deficiency Leads to Greater Depletion and Activation of HDC+ MB-HSCs in DSS-Induced Colitis

Given that HDC is the key gene required for histamine production, and is required for maintaining normal MB-HSC quiescence, we hypothesized that knockout of the HDC gene might lead to greater activation and depletion of MB-HSCs in the setting of DSS colitis. We used HDC-/-; HDC-GFP mice that were used in our previous study to investigate the impact of HDC deficiency on DSS colitis. We found that DSS colitis in HDC-/-; HDC-GFP mice resulted in a much more severe colonic injury on day 3 and day 5 ($P < .01$), based on histologic scoring of H&E-stained sections (Figure 4*A*), and there was no significant increase of the histologic score of HDC-/-; HDC-GFP mice compared with HDC-GFP mice on d7. In addition, body weights in HDC-/-; HDC-GFP mice showed a greater reduction on day 6 ($P < .05$) (Figure 4*B*), and overall survival was decreased ($P = .0451$) (Figure 4*C*) compared with wild-type (WT) HDC-GFP mice.

Furthermore, we analyzed the effect of HDC gene deficiency on the HDC+ MB-HSCs in both the bone marrow and spleen. In the bone marrow, HDC-/-; HDC-GFP mice showed a significant decrease in total number on d7 ($P < .05$) (Figure 4*D*), and the percentage of HDC+ HSCs among total HSCs (Figure 4*E*) was decreased from day 1 to day 7 ($P < .05$). Similarly, in the spleen, the total number of HDC+ HSCs was decreased in HDC-/-; HDC-GFP mice on d5 and d7 ($P < .01$ on d5 and $P < .05$ on d7) (Figure 4*F*), and the percentage of HDC+ HSCs among HSCs in the spleen was decreased from day 1 to day 5 compared with HDC-GFP mice ($P < .05$ on d1 and d5; $P < .01$ on d3) (Figure 4*G*). In cell-cycle analysis, we found that DSS-treated HDC knockout mice had a lower percentage of HSCs ($P < .01$) (Figure 4*H* and *I*) and HSPCs ($P < .01$) (Figure 4*H* and I) in a quiescent G0 state on day 5 compared with DSS-treated HDC-GFP mice. Furthermore, the percentage of BrdU+ HDC+ HSCs in HDC-/-; HDC-GFP mice was 1.3-fold increased on d5 and d7 compared with HDC-GFP mice ($P < .05$, respectively) (Figure 4*J*).

## HDC Deficiency Promotes Greater Recruitment of HDC+ Myeloid Cells to the Colon in DSS-Induced Colitis

Because BM HDC+ HSCs in HDC-deficient mice showed much greater activation than in WT mice, based on greater BrdU uptake and a lower percentage of cells in G0, we next studied the impact of this activation on myeloid cell production. Thus, we found that in DSS-treated HDC-deficient mice, the percentage of BM GFP+ myeloid cells among CD45+ cells were increased at all time points compared with HDC-GFP mice ($P < .05$ on d1 and d7; $P < .01$ on d3 and d5) (Figure 4*K*). In addition, the percentage of HDC+ myeloid cells among CD45+ cells in the spleen of DSS-treated HDC-deficient mice was increased on d3 and d5 ($P < .05$) (Figure 4*L*) compared with HDC-GFP mice. Similarly, in the circulation, the percentage of HDC+ myeloid cells among CD45+ cells ($P < .01$ on d7) (Figure 4*M*) increased from d1 to d7, with up to a 1.4-fold increase on d7 in circulation. Likewise, in the colon, immunofluorescence staining (Figure 4*N*) showed a marked increase in HDC+ myeloid cell recruitment in HDC-/-; HDC-GFP mice compared with HDC- GFP mice ($P < .05$ on d5 and d7) (Figure 4*O*). Taken together, HDC deficiency alters the response by MB-HSCs to DSS colitis, resulting in much greater activation of HDC+ HSCs and greater recruitment of daughter myeloid cells into the circulation and injured colon. Importantly, by d7 this increased production appears to abate, suggesting the early onset of HDC+ HSC exhaustion.

## Depletion of HDC+ Myeloid Cells Leads to Greater HDC+ MB-HSC Activation and Then Exhaustion

The earlier-described studies suggested that HDC+ myeloid cells are important niche cells, and that reductions

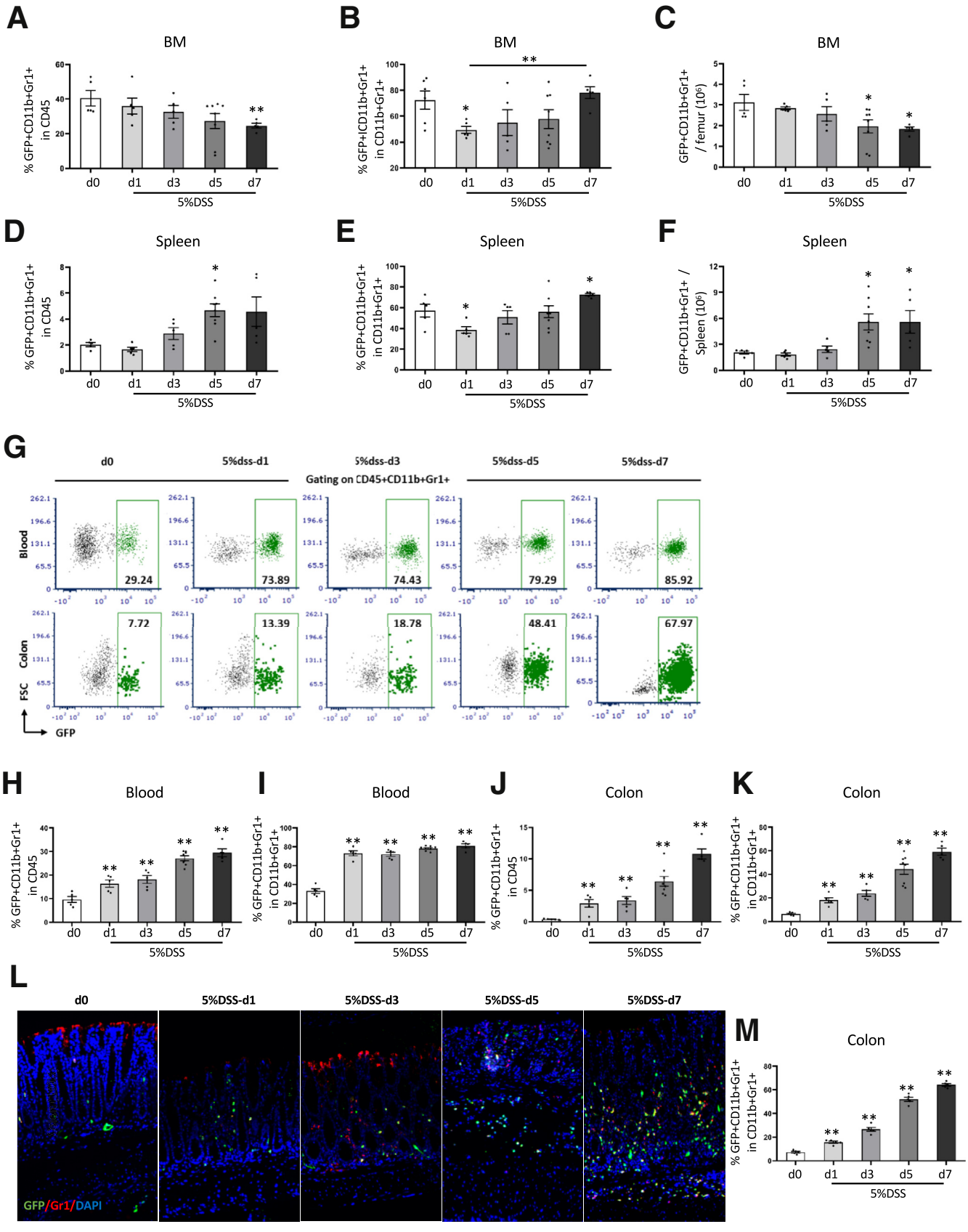
A
BM
% GFP+CD11b+Gr1+ in CD45
d0 d1 d3 d5 d7
5%DSS
B
BM
% GFP+CD11b+Gr1+ in CD11b+Gr1+
C
BM
GFP+CD11b+Gr1+ / femur (10^6)
D
Spleen
E
Spleen
F
Spleen
GFP+CD11b+Gr1+ / Spleen (10^6)
G
d0
5%dss-d1
5%dss-d3
5%dss-d5
5%dss-d7
Gating on CD45+CD11b+Gr1+
Blood
Colon
FSC
GFP
29.24
73.89
74.43
79.29
85.92
7.72
13.39
18.78
48.41
67.97
H
Blood
I
Blood
J
Colon
K
Colon
L
d0
5%DSS-d1
5%DSS-d3
5%DSS-d5
5%DSS-d7
GFP/Gr1/DAPI
M
Colon

in bone marrow histamine-secreting myeloid cells during DSS colitis correlates with greater activation of HDC+ MB-HSCs. To test the role more directly of HDC+ myeloid cells in protecting HDC+ MB-HSCs during DSS colitis, we used the inducible diphtheria toxin receptor (iDTR) to deplete HDC+ myeloid cells (Figure 5*A*). We previously showed that treatment of HDC-GFP; HDC–tamoxifen-inducible recombinase Cre system (CreERT); iDTR mice with DT depletes only HDC+ myeloid cells (which highly express HDC-DTR), but not HSCs or HSPCs (which show low levels of HDC-DTR expression).[14] Controls for this study included DTR- mice treated with DT. Compared with DTR- mice, DTR+ mice treated with tamoxifen, then DT, and then DSS showed a marked decrease (approximately 50%) in the percentage of HDC+ myeloid cells among CD45+ cells ($P < .01$) (Figure 5*C*); and among CD11b+Gr1+ cells ($P < .01$) (Figure 5*B* and *D*) in the circulation. The percentage in the spleen of HDC+ CD11b+Gr1+ cells among CD45+ cells ($P < .01$) (Figure 5*E*) and among total CD11b+Gr1+ myeloid cells ($P < .01$) (Figure 5*B* and *F*) also were decreased in DTR+ mice compared with DTR- mice. In addition, in the colon, the percentage of HDC+ CD11b+Gr1+ cells among CD45+ cells ($P < .01$) (Figure 5*G*) and among total CD11b+Gr1+ myeloid cells ($P < .01$) (Figure 5*B* and *H*) also were decreased in DTR+ mice compared with DTR- mice, which was reflected in the decreased colonic infiltration by HDC+ myeloid cells as seen by immunofluorescence ($P < .01$) (Figure 5*I* and *J*). These results showed the efficiency of DTR-mediated HDC+ myeloid cell depletion.

Furthermore, the percentage in the bone marrow of HDC+ CD11b+Gr1+ cells among CD45+ cells ($P < .01$) (Figure 5*K*) and among CD11b+Gr1+ cells ($P < .01$) (Figure 5*L*) also was decreased in DT-treated DTR+ mice. We found in the bone marrow that DTR-mediated HDC+ myeloid cell depletion led to a marked decrease in the percentage of HDC+ HSCs among lineage-negative cells ($P < .01$) (Figure 5*M*) and the total number of HDC+ HSCs ($P < .05$) (Figure 5*N*). The activation and proliferation of BM HDC+ HSCs of DTR+ mice were notably increased, as evidenced by a decreased percentage of G0 cells ($P < .01$) (Figure 5*O*) and increased percentage of BrdU+ cells ($P < .01$) (Figure 5*P*) in DT-treated HDC+ HSCs. These findings all are consistent with activation and exhaustion of the HDC+ HSCs after depletion of HDC+ myeloid cells. Importantly, the DT-treated DTR+ mice showed a notable decrease in body weight compared with DTR- mice ($P < .05$ on d2 and d3) (Figure 5*Q*), and also significantly worse overall survival ($P = .0371$) (Figure 5*R*). However, there were no significant changes in the degree of colon injury according to histologic assessment and scoring ($P > .05$, Figure 5*S* and *T*), suggesting that the reduced survival of DT-treated DTR+ mice might be more related to MB-HSC depletion and exhaustion than to colitis alone.

## H2R Agonist Preserves the Quiescence of HDC+ MB-HSCs and Improve Outcomes in DSS-Induced Acute Colitis

Previous studies have suggested that in addition to a deficiency in histamine, the activation and exhaustion of MB-HSCs can be triggered by an endotoxin (LPS) through a TLR4 pathway.[14] Thus, we tested whether either a TLR4 antagonist eritoran tetrasodium (E5564)[28] or a H2R agonist could provide protection in DSS models of colitis. We examined these interventions in 2 models: both our standard DSS-induced model (Figure 6*A*) and a previously published model[29] that combines 4 antibiotics (ABX) plus DSS (4-ABX + DSS model) (Figure 6*B*), which is another colitis model characterized by severe weight loss, colonic bleeding, and colonic shortening. The H2R agonist dimaprit dihydrochloride was able to suppress the marked decrease in body weight (Figure 6*C* and *E*) and also increase overall survival ($P = .0177$, $P = .0492$, respectively) (Figure 6*D* and *F*) of mice in both models. However, the TLR4 antagonist E5564 was able to only attenuate weight loss and improve survival of mice in the DSS-induced model ($P = .0282$) (Figure 6*C* and *D*), but not improve survival of the 4-ABX + DSS model ($P = .7342$) (Figure 6*E* and *F*). In addition, the combination of the H2R agonist and the TLR4 antagonist was able to attenuate weight loss and increase the overall survival of mice in both the DSS-induced model ($P = .0397$) (Figure 6*C* and *D*) and the 4-ABX + DSS model ($P = .0347$) (Figure 6*E* and *F*). Together, these studies indicated that the H2R agonist dimaprit dihydrochloride appears most effective in ameliorating acute colitis. Time-course studies confirmed the potential protective role of the H2R agonist on DSS colitis (Figure 6*G*), with a decreased ratio of spleen weight to body weight with H2R agonist treatment compared with phosphate-buffered saline (PBS) treatment ($P < .05$ on d5 and d7) (Figure 6*H*). Although the histologic injury remained severe from d5 to d7 (Figure 6*I*), the histologic score was improved in the H2R-agonist treatment

**Figure 3.** (***See previous page***). **HDC+ myeloid cells were derived from BM into circulation and recruited in the colon.** Comparison of the percentage of BM GFP+ myeloid cells among (*A*) CD45+ cells and (*B*) myeloid cells from different time points of 5% DSS treatment. (*C*) Number of GFP+ myeloid cells in BM from different time points of 5% DSS treatment. Comparison of percentage of splenic GFP+ myeloid cells among (*D*) CD45+ cells and (*E*) myeloid cells from different time points of 5% DSS treatment. (*F*) Number of GFP+ myeloid cells in the spleen from different time points of 5% DSS treatment. (*G*) FACS plots showed the percentage of GFP+ myeloid cells in blood and in the colon from different time points of 5% DSS treatment. Percentage of GFP+ myeloid cells among (*H*) CD45+ cells and the (*I*) total myeloid cells in the blood from different time points of 5% DSS treatment. Percentage of GFP+ myeloid cells among (*J*) CD45+ cells and the (*K*) total myeloid cells in the colon from different time point of 5% DSS treatment. (*L*) Immunofluorescent images showing GFP+Gr1+ cells in the colon at different time points of 5% DSS treatment. (*M*) Quantification of the percentage of GFP+ Gr1+ cells among all GFP+ cells. Data are expressed as means ± SEM. Results are representative of at least 3 independent experiments. **P* < .05, ***P* < .01. DAPI, 4′,6-diamidino-2-phenylindole.

group compared with the control group on d3 ($P < .05$) (Figure 6*J*).

Importantly, the H2R agonist dimaprit showed a significant increase in the percentage of GFP+ MB-HSCs among bone marrow lineage-negative cells ($P < .01$ on d7) (Figure 7*A*) and among total HSCs ($P < .05$ on d7) (Figure 7*B*), and also in the total number of HDC+ HSCs on day 5 and day 7 ($P < .05$ on d5 and $P < .01$ on d7) (Figure 7*C*). Similarly, in the spleen, the percentage of GFP+ HSCs among lineage-negative cells ($P < .01$ on d5 and d7) (Figure 7*D*) and the total number of GFP+ HSCs ($P < .01$ on d5 and d7) (Figure 7*F*) were increased on day 5 and day 7, although the percentage of GFP+ HSCs among total HSCs was increased only on day 7 ($P < .05$) (Figure 7*E*). In our

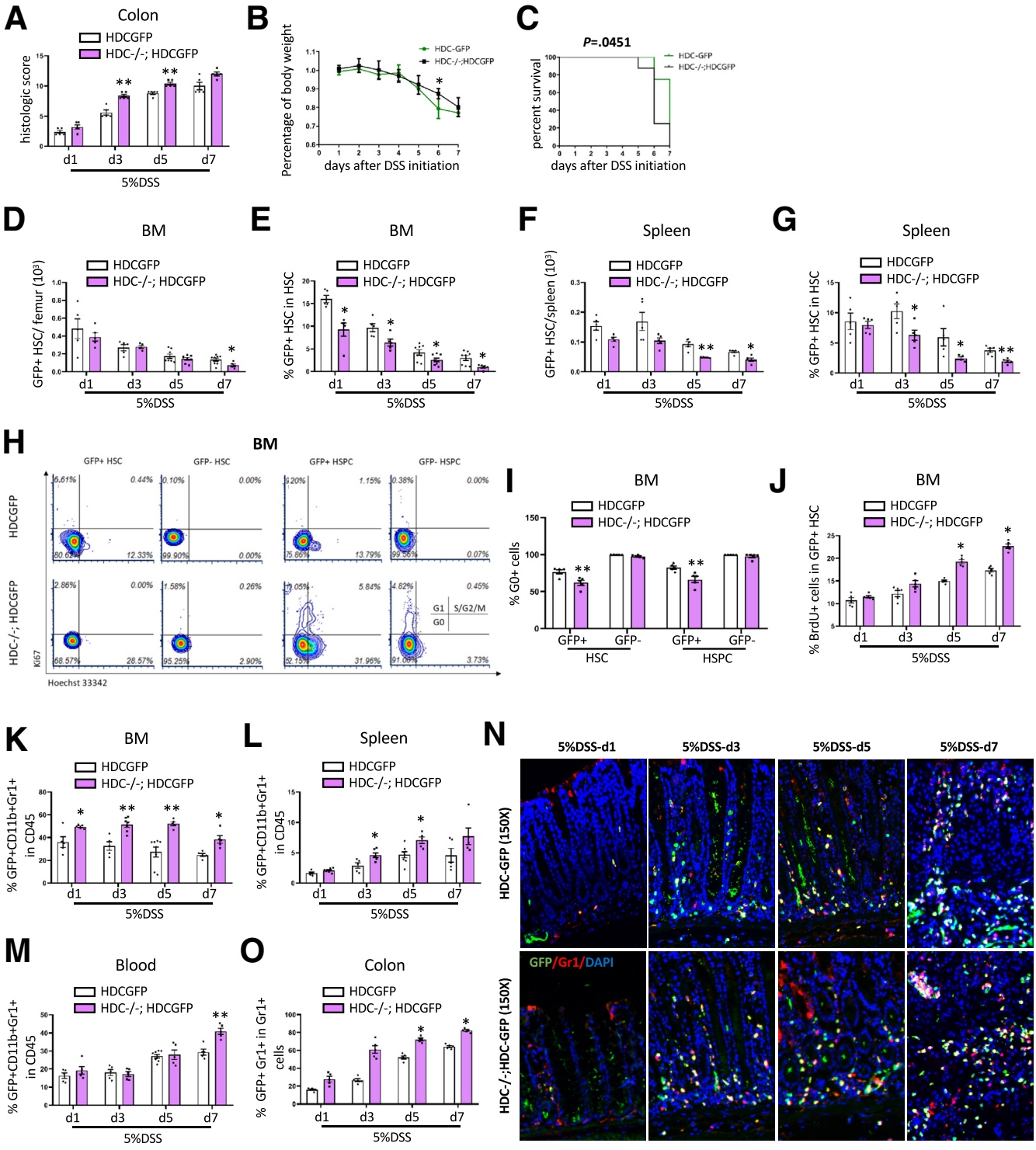

cell-cycle analysis, we found that treatment with the H2R agonist resulted in a higher percentage of G0 among HDC+ MB-HSCs ($P < .01$) (Figure 7*G* and *H*) on day 5 after DSS initiation compared with control mice. Furthermore, the percentage of BrdU+ cells among HDC+ HSCs in H2R-agonist–treated mice was decreased at all time points (39%, 30%, 23%, and 18%, respectively) compared with control mice ($P < .01$ on d1, d5, and d7; $P < .05$ on d3) (Figure 7*I*). Taken together, these data indicate that the H2R agonist, dimaprit, is able to preserve the quiescent HDC+ MB-HSCs and improve outcomes in DSS-induced acute colitis.

Interestingly, we also noted that the percentage of HDC+ myeloid cells among the CD45+ cells in the BM were increased in the H2R agonist treatment group compared with the control group on d7 ($P < .05$ on d7) (Figure 8*A*). In particular, the total number of HDC+ myeloid cells in BM was 1.5-fold increased on d7 ($P < .01$ on d7) (Figure 8*B*). In contrast, in the spleen, the percentage of HDC+ myeloid cells among the CD45+ cells ($P < .05$) (Figure 8*C*) and the total number of HDC+ myeloid cells were approximately 2-fold increased on d1 ($P < .05$ on d7) (Figure 8*D*). Furthermore, the percentage of HDC+ myeloid cells among CD45+ cells ($P < .05$ on d5 and d7) (Figure 8*E*) and among the whole myeloid cells ($P < .05$ on d7) (Figure 8*F*) in the blood showed a decrease in the H2R-agonist treatment group compared with the control group. Finally, in the colon, we found the percentage of HDC+ myeloid cells among CD45+ cells ($P < .05$ on d5; $P < .01$ on d7) (Figure 8*G*) and among the whole myeloid cells ($P < .05$ on d7) (Figure 8*H*) were decreased in the H2R-agonist treatment group after DSS treatment. We found overall decreased infiltration in the colon by HDC+ myeloid cells as shown by immunofluorescence imaging of frozen colon tissue from H2R-agonist–treated HDC-GFP mice on d5 and d7 ($P < .01$ on d5; $P < .05$ on d7) (Figure 8*I* and *J*). The H2R agonist dimaprit also was able to significantly attenuate body weight loss ($P < .05$ on d5) (Figure 8*K*) and improve survival ($P = .0177$) (Figure 8*L*) of mice with DSS-induced colitis.

Furthermore, to evaluate the role of H2R agonist on the overall level of colonic inflammation, we performed a quantitative reverse-transcription polymerase chain reaction (qRT-PCR) mRNA array to assess the expression of a panel of cytokines and chemokines. We found in the spleens from H2R-treated C57BL/6 mice with DSS colitis on d7 that among 84 cytokine/chemokine genes, there were 10 genes up-regulated and 74 genes down-regulated (Table 1), suggesting a largely anti-inflammatory response. Among down-regulated genes, interleukin (IL)6 mRNA ($P < .01$) (Figure 8*M*) and colony-stimulating factor (csf) 2 mRNA ($P < .01$) (Figure 8*N*) were verified by qRT-PCR and showed a significant decrease in the spleens of H2R-agonist–treated mice. Because IL6 is expressed primarily and secreted by monocytes/macrophages, we analyzed this subset of myeloid cells (Figure 8*O*) using flow cytometry. We found no significant change in the percentage of monocytes (CD11b+Ly6G- Ly6C+F4/80-) and macrophages (CD11b+Ly6G- Ly6C-F4/80+) in the spleen between the PBS control group and the H2R-agonist group (Figure 8*P* and *Q*). Thus, although H2R agonist was able to preserve quiescence of the HDC+ MB-HSCs, reduce inflammatory cytokines, and improve outcomes in DSS-induced acute colitis, it did not impair overall myeloid cell production or reduce the requisite myeloid cell response[30] previously shown to contribute to colonic healing.

## Discussion

Here, we used HDC transgenic mice (HDC-GFP, HDC-/-, and HDC-CreERT2) in DSS-induced colitis, a well-established model of acute colonic mucosal inflammation,[31] to explore the role of histamine-secreting myeloid niche cells in the regulation of MB-HSCs and in response to severe colitis. We found that in response to colonic injury and inflammation demand, HDC+ myeloid cells rapidly exit the bone marrow, leading to loss of the quiescent histamine niche signal, rapid cycling of HSCs, and rapid myeloid cell production. Thus, over time, severe inflammatory stress can trigger MB-HSC depletion with adverse clinical outcomes, but treatment with H2R agonists can prevent MB-HSC exhaustion. Our finding adds to the growing evidence regarding the contribution of MB-HSCs to DSS-induced acute colitis, and further reinforces the feedback regulatory role of bone marrow HDC+ myeloid cells on MB-HSCs through the histamine/H2R axis.

The critical role of HSCs has been well established in both intestinal infection and inflammation, which can place

**Figure 4.** (***See previous page***). **HDC deficiency leads to greater depletion and activation of MB-HSCs in DSS-induced acute colitis and promotes greater recruitment of HDC+ myeloid cells in the colon.** (*A*) Comparison of the severity of DSS-induced acute colitis in HDC-/-; HDC-GFP mice, and HDC-GFP mice were evaluated by histopathologic scoring of H&E-stained slides. (*B*) Analysis of body weight change and (*C*) Kaplan–Meier curve depicting survival rates of HDC-GFP mice and HDC-/-; HDC-GFP mice at different time points of 5% DSS treatment. Total number of (*D*) BM GFP+HSCs and the (*E*) percentage of GFP+ HSCs among total HSCs from HDC-/-; HDC-GFP mice compared with HDC-GFP mice at different time points of 5% DSS treatment. Total number of (*F*) splenic GFP+ HSCs and the (*G*) percentage of GFP+ HSCs among total HSCs from HDC-/-; HDC-GFP mice compared with HDC-GFP mice at different time points of 5% DSS treatment. (*H*) Cell-cycle analysis with FACS for Ki67 and Hoechst 33342 staining and the (*I*) percentage of G0 cells of BM HSCs and HSPCs from HDC-GFP mice and HDC-/-; HDC-GFP mice at 5 days after 5% DSS treatment. (*J*) Percentage of BrdU+ cells of BM GFP+ HSCs of HDC-/-; HDC-GFP mice compared with HDC-GFP mice at different time points of 5% DSS treatment. Percentage of GFP+ myeloid cells among CD45+ cells in (*K*) BM, (*L*) spleen, and (*M*) blood of HDC-GFP mice and HDC-/-; HDC-GFP mice at different time points of 5% DSS treatment. (*N*) Immunofluorescent images showing GFP+Gr1+ cells in the distal colon from HDC-GFP mice and HDC-/-; HDC-GFP mice at different time points of 5% DSS treatment. (*O*) Quantification of the percentage of GFP+ Gr1+ cells among all GFP+ cells. Data are expressed as means ± SEM. Results are representative of at least 3 independent experiments. *$P < .05$, **$P < .01$. DAPI, 4′,6-diamidino-2-phenylindole.

great demands on HSCs to quickly produce immune effector cells.[32] DSS-induced colitis leads to an acute gut injury, and has been one of the most commonly used mouse models for IBD.[31] Hematopoietic cells, and, in particular, HSCs, are central to IBD, as evidenced by the occasional use of HSC transplantation to treat patients with Crohn's disease.[33] Griseri et al[34] reported that deregulated HSCs and progenitor cell activity could lead to IL23-driven chronic intestinal inflammation. Nevertheless, the role and regulation of HSCs during DSS-induced acute colitis is poorly characterized.

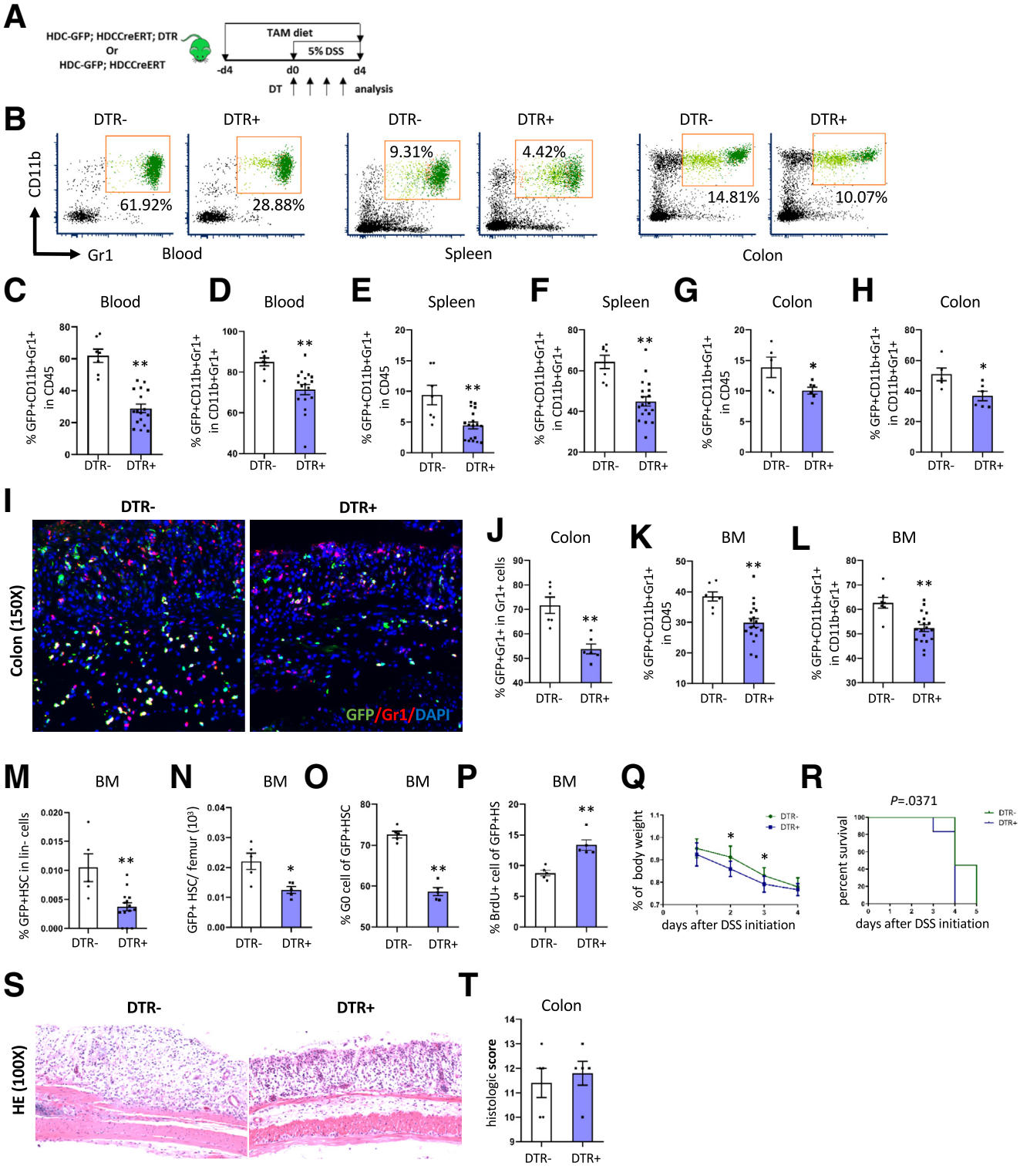

Similar to our earlier study, we found that HDC marked a subset of HSCs, which gave rise to HDC+ myeloid cells and thus were defined as MB-HSCs.[14] However, the hematopoietic hierarchy normally present in homeostatic conditions was markedly impaired under conditions of acute colitis because HDC+ HSCs decreased rapidly in the BM and were nearly exhausted with the progression of DSS-induced acute colitis. HDC+ HSC proliferation was increased substantially during acute colitis and correlated with a sustained transition into MPP3. This activation of MB-HSCs led to a subsequent increase of the frequency of CD11b+Gr1+ myeloid cells in the BM, thus replenishing the BM myeloid pool in response to the demand for myeloid cells in the setting of severe inflammation. Similarly, HDC+ HSCs in acute colitis were activated and depleted in extramedullary sites such as the spleen at the late stage, possibly related to the failure of the BM to respond adequately to severe inflammatory stress. Thus, the inflamed spleen constitutes a reservoir of HSCs and granulocyte-macrophage progenitors that can contribute to myeloid cell production, which have been shown to migrate to the colon during IL23-driven chronic colitis.[34] Several studies[35,36] also have shown that compared with BM, splenic HSCs displayed a pre-activated phenotype, which may expedite their cell-cycle entry in emergency conditions. However, in our DSS colitis model, we found HDC+ HSCs in BM were decreased significantly and then mostly restored in the recovery phase (data not shown), indicating that HDC+ HSC exhaustion in BM is a feature of acute, severe DSS colitis. To date, there is no evidence as to the role of HDC+ HSCs in other types of murine colitis models, such as the hapten-induced colitis model in which lymphoid cells play a more predominant role.[37] Thus, one important limitation of our study was that we used only 1 murine model of IBD, characterized by mucosal injury and innate immune responses, which may differ in important ways from human IBD.[24,38,39] Further studies are needed to clarify the role of HDC+ HSCs in other murine colitis models (eg, 2, 4, 6-Trinitrobenzene Sulfonic Acid (TNBS)-induced colitis and IL10 knockout model).[40–42]

HSCs are not only regulated by inflammatory demands, but also are direct targets of myeloid-derived inflammatory signaling,[32] such as interferons,[43] tumor necrosis factor,[44] and TLR ligands,[45] in part because of the expression of receptors for these microbial products and inflammatory cytokines.[46,47] Indeed, inflammatory signals can alter the bone marrow microenvironment, which indirectly can influence the activity and fate of HSCs. Stromal cells that populate these stem cell niches provide essential signals to HSCs that regulate their proliferation, differentiation, and retention in the bone marrow. In our previous study, we showed that HDC+ MB-HSCs resided in the center of a cluster of mature HDC-expressing myeloid cells, niche cells that served as the major source of histamine in the BM, which we showed to be necessary for maintaining the quiescence and self-renewal of MB-HSCs.[14] During progression of acute colitis, the total number of HDC+ CD11b+Gr1+ myeloid cells in the BM was diminished because they exited the bone marrow into the circulation, and accumulated rapidly in the colon, presumably to aid in the repair and regeneration of the intestine.[30] Bone marrow–derived myeloid cells played a key role in the response to radiation and LPS-induced intestinal injury, serving as the first responder to defend infection,[14] and removed cellular debris. Thus, in response to acute colitis, HDC+ CD11b+Gr1+ myeloid cells were depleted rapidly from the BM, generating a deficit in histamine signaling, the critical regulatory factor to prevent activation of MB-HSCs from their normal quiescent state.

The importance of the deficit in histamine signaling in disease progression in acute colitis was underlined by our studies here with HDC knockout mice, lacking HDC gene expression, and HDC- CreERT; iDTR mice, which when induced and treated with DT injection show a paucity of HDC-expressing myeloid cells.[1,14] HDC deficiency led to increased proliferation and eventual exhaustion of HDC-GFP+ HSCs. The activation of bone marrow MB-HSCs resulted in increased myeloid-biased MPP3 and eventually increased production of HDC+ myeloid cells. Depleting bone marrow HDC+ CD11b+Gr1+ myeloid cells after diphtheria toxin administration similarly depleted histamine signaling in the bone marrow, enforced cell-cycle entry, and resulted in eventual exhaustion of MB-HSCs. These interventions appeared to sensitize animals to acute DSS-induced colitis because these cycling MB-HSCs failed to revert into quiescence in the absence of histamine feedback, which impacted overall survival. Survival analysis of HDC-/- mice and DTR+

**Figure 5.** (***See previous page***). **Depletion of HDC+ myeloid cell leads to greater HDC+ MB-HSC exhaustion.** (*A*) The treatment protocol for depleting HDC+ myeloid cells in HDC-GFP; HDCCreERT; DTR mice. (*B*) FACS plots showing myeloid cells in blood, spleen, and colon from DTR+ and DTR- mice. Percentage of GFP+ myeloid cells among CD45+ cells and among the total myeloid cells in the (*C*) blood and (*D*) colon from different DTR+ and DTR- mice. Percentage of GFP+ myeloid cells among CD45+ cells and among the total myeloid cells in the (*E*) spleen and (*F*) colon from different DTR+ and DTR- mice. Percentage of GFP+ myeloid cells among CD45+ cells and among the total myeloid cells in the (*G*) colon and (*H*) colons from different DTR+ and DTR- mice. (*I*) Immunofluorescent images showing GFP+Gr1+ cells in the colon of DTR+ and DTR- mice. (*J*) Quantification of the percentage of GFP+ Gr1+ cells among all GFP+ cells. Comparison of the percentage of BM GFP+ myeloid cells among (*K*) CD45+ cells and (*L*) myeloid cells from DTR+ and DTR- mice. Percentage of GFP+ HSCs among (*M*) lineage-negative cells and (*N*) LSK from DTR+ and DTR- mice. (*O*) Cell-cycle analysis with FACS for Ki67 and Hoechst 33342 staining and the percentage of G0 cells of BM GFP+ HSCs from DTR+ mice compared with DTR- mice. (*P*) Percentage of BrdU+ cells of BM GFP+ HSCs from DTR+ mice compared with DTR- mice. (*Q*) Analysis of body weight change between DTR+ mice and DTR- mice. (*R*) Kaplan–Meier curve depicting survival rates of DTR+ mice and DTR- mice. (*S*) Representative histologic images of injured colon by H&E staining from DTR- and DTR+ mice and the (*T*) colitis severity grade as evaluated by histopathologic scores. Data are expressed as means ± SEM. Results are representative of at least 3 independent experiments. $^{*}P < .05$, $^{**}P < .01$. DAPI, 4′,6-diamidino-2-phenylindole.

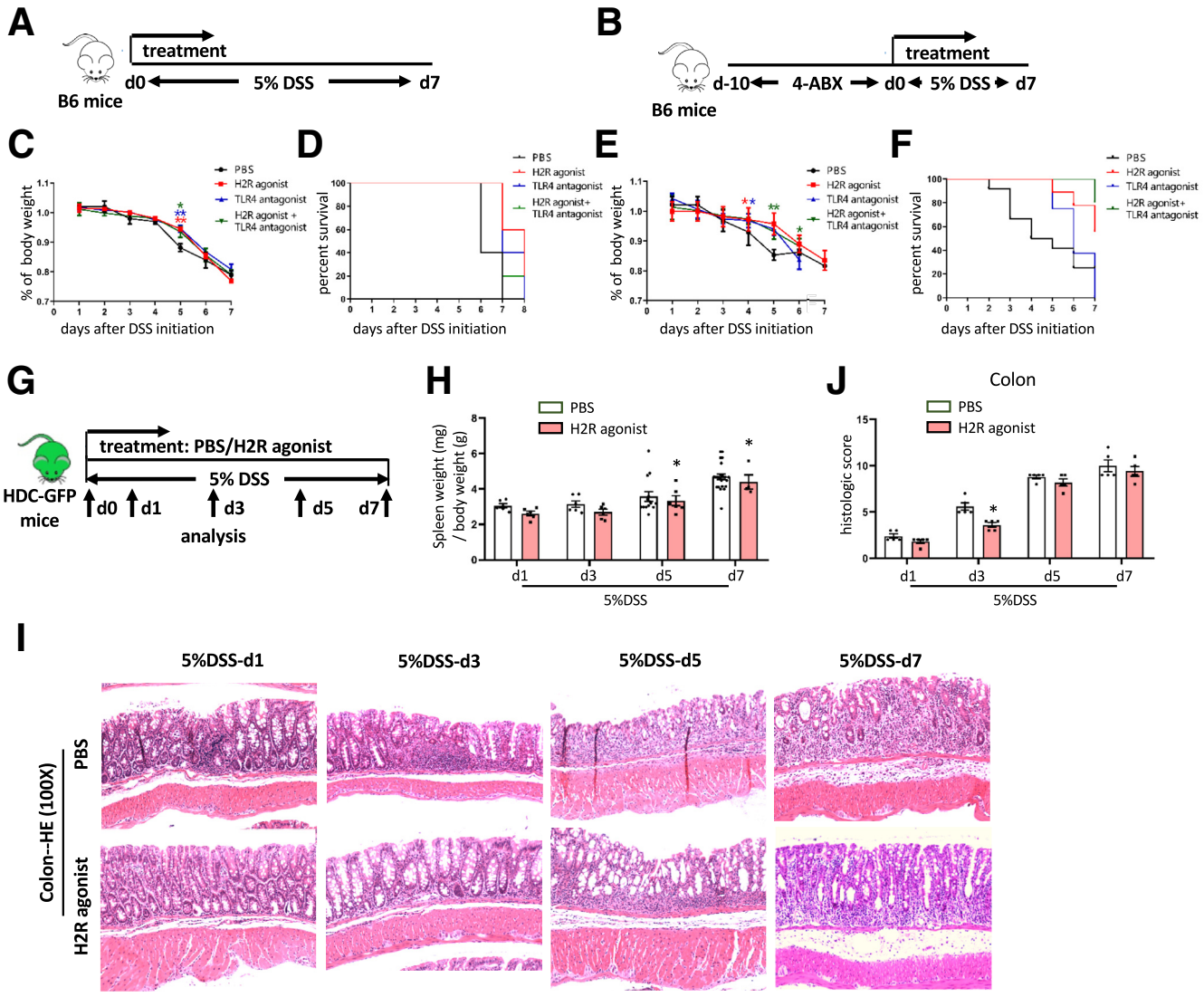


**Figure 6. H2R agonist increases the survival in B6 WT mice treated with DSS or 4-ABX + DSS and improves outcomes in DSS-induced acute colitis.** Treatment protocol of B6 mice with (*A*) DSS-induced and (*B*) 4-ABX + DSS–induced acute colitis. (*C*) Analysis of body weight change and (*D*) Kaplan–Meier curve depicting survival rates of B6 mice with DSS-induced colitis between the H2R agonist–treated group and the PBS group. (*E*) Analysis of body weight change and (*F*) Kaplan–Meier curve depicting survival rates of B6 mice with 4-ABX + DSS–induced colitis between the H2R agonist–treated group and the PBS group. (*G*) Treatment protocol of HDC-GFP mice with DSS-induced acute colitis. (H) Analysis of the ratio of spleen weight to body weight of HDC-GFP mice treated with DSS between the H2R agonist–treated and the PBS group. (*I*) The severities of DSS-induced acute colitis were observed by H&E staining and (*J*) were evaluated by histologic scores between the H2R agonist–treated and the PBS group. Data are expressed as means ± SEM. Results are representative of at least 3 independent experiments. $^{*}P < .05$, $^{**}P < .01$.

mice all showed shorter life survival compared with the relative control mice, which could be owing in part to a greater sensitivity of MB-HSCs to DSS.

Because the loss of quiescence by MB-HSCs, owing either to knockout of the HDC gene or ablation of the HDC+ myeloid descendants, appeared to worsen the outcome of mice with acute DSS colitis, we tested the therapeutic benefit of promoting MB-HSC quiescence using a histamine agonist. There are 4 histamine receptors—H1R, H2R, H3R, and H4R—and among the 4 known histamine receptors, only H2R was detectable on both HSCs and progenitors.[14] We selected the H2R-agonist dimaprit for our study to examine further the protective role of H2R signaling in DSS-induced acute colitis. First, the H2R selective agonist dimaprit is a highly specific agonist and almost as active as the endogenous ligand histamine at the H2R.[48] Second, the finding of increased expression of H2R on HDC-GFP$^{hi}$ MB-HSCs[14] also raised the possibility that these cells might be intrinsically more responsive to histamine. Thus, we found that this exogenous H2 agonist, dimaprit, was able to protect MB-HSCs from becoming exhausted, and was able to maintain the quiescent status

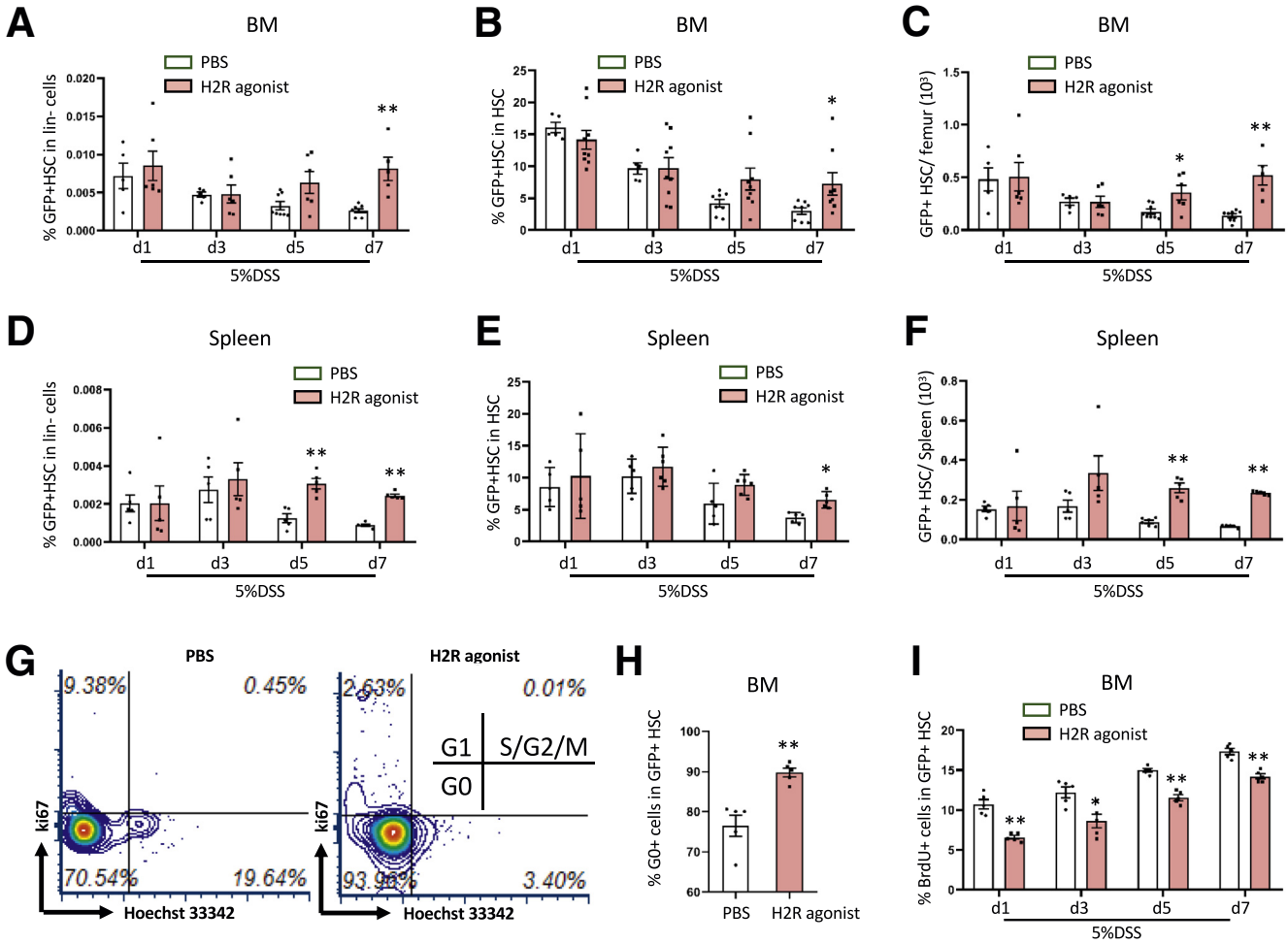


**Figure 7. H2R agonist preserves the quiescent MB-HSCs and improves outcomes of DSS-induced acute colitis.** Comparison of the percentage of GFP+ HSCs among (*A*) lineage-negative cells and (*B*) HSCs from the H2R agonist–treated group and the PBS group. (*C*) Number of BM GFP+ HSCs from different time points of 5% DSS treatment. Comparison of the percentage of GFP+ HSCs among (*D*) lineage-negative cells and (*E*) HSCs, and the (*F*) number of GFP+ HSCs from spleen at different time points of 5% DSS treatment. (*G*) Cell-cycle analysis with FACS for Ki67 and Hoechst 33342 staining and the (*H*) percentage of G0 cells of BM HSCs and HSPCs at 5 days after the H2R agonist–treated group and the PBS group. (*I*) Percentage of BrdU+ cells of BM GFP+ HSCs from the H2R agonist–treated group and the PBS group. Data are expressed as means ± SEM. Results are representative of at least 3 independent experiments. *$P < .05$, **$P < .01$.

of reserve MB-HSCs in the setting of acute DSS-induced colonic injury. In addition, we found that dimaprit treatment was able to improve the overall survival of mice with acute DSS-induced colitis. It is important to note that previous animal studies have noted increases in mucosal histamine in models of IBD, and noted some potential benefits of the H2R antagonist in DSS rodent models and IBD patients.[49] However, these data as a whole were highly heterogeneous, focused primarily on mast cells and the intestinal mucosa, and failed to examine effects on bone marrow or assess overall survival. Although more recent studies have focused on the role of H4R in driving neutrophil recruitment and the severity of colitis,[50] it is clear that further studies are needed to clarify the role and clinical importance of the histamine–H2R axis.

The H2 agonist dimaprit also suppressed the accumulation of HDC+ myeloid cells in the colon and decreased the productions of cytokines such as IL6 and csf1 mRNA expression in the spleen. IL6 is a prominent proinflammatory cytokine that plays a critical role in modulating immunity and inflammation,[51,52] and also regulates the proliferation and differentiation of HSCs.[53] Interestingly, we found that H2R-agonist treatment reduced the level of IL6 in the circulation, spleen, and colon, and suppressed the activation of HSCs, leading to improved survival of mice with severe colitis. HSC differentiation is induced by the cytokine granulocyte-macrophage colony-stimulating factor (GM-CSF), which is thought to drive HSCs to differentiate into common myeloid progenitors.[54] GM-CSF also promote both the proliferation and survival of granulocyte-macrophage progenitors.[55] We found that the H2R agonist decreased the levels of GM-CSF in acute DSS colitis, which also might contribute to the survival of mice with DSS-induced acute colitis. IL6 was mainly synthesized and secreted by monocytes/macrophages,[56,57] but we found no significant change in the percentage of monocytes and macrophages with dimaprit treatment.

In summary, acute DSS colitis leads to a loss of quiescence by MB-HSCs in bone marrow, leading to activation and extensive HDC+ myeloid cell production, and, eventually, bone marrow stem cell exhaustion, which impacts survival. The level of HDC expression modulates this response, with HDC deficiency leading to more rapid HDC+ MB-HSC activation and depletion, with worse outcomes. Treatment with an H2R agonist is able to improve

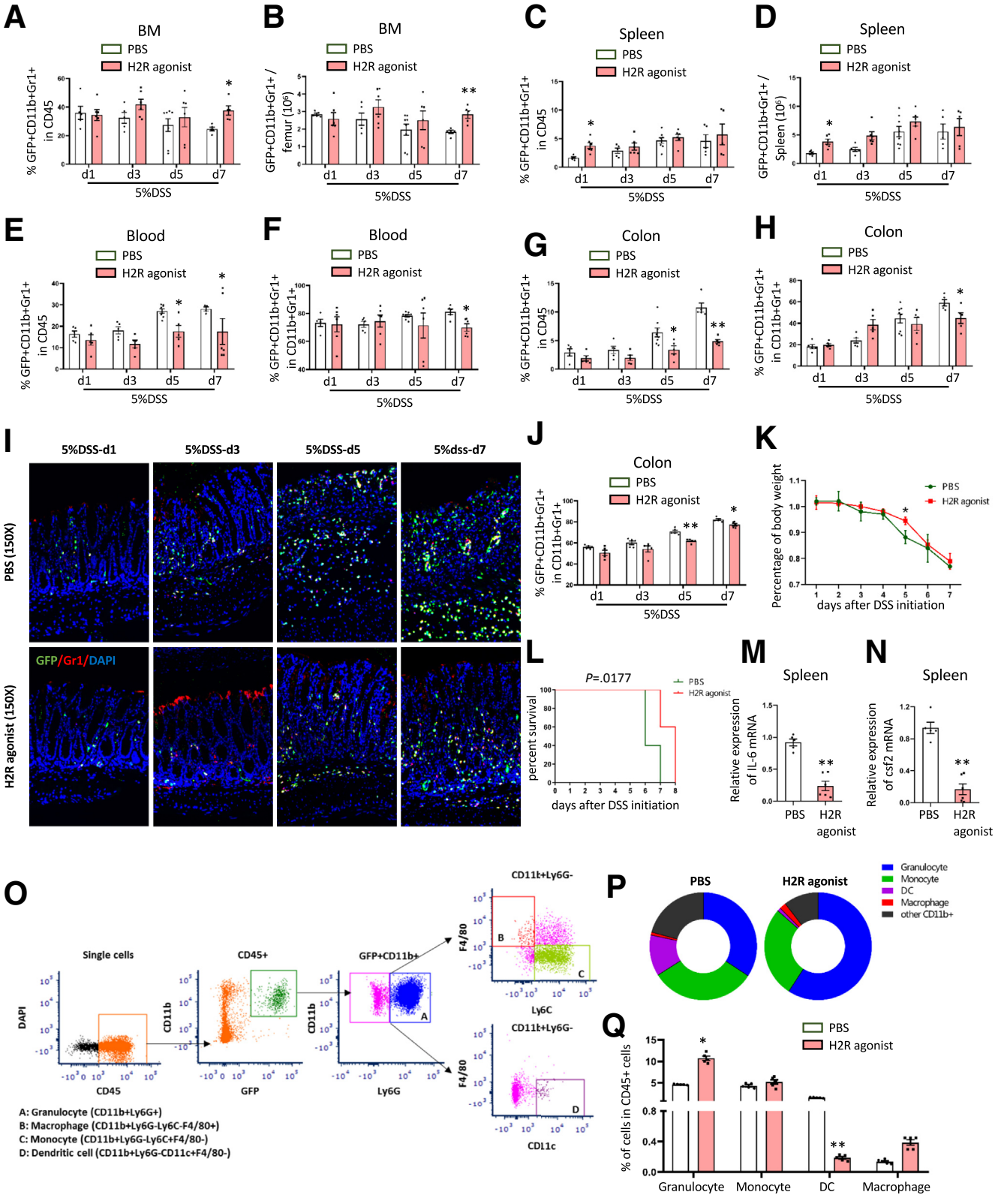

**Table 1.** The Raw Data of Cytokine and Chemokine qRT-PCR Array

| Symbol | Fold regulation | Symbol | Fold regulation | Symbol | Fold regulation | Symbol | Fold regulation |
|---|---|---|---|---|---|---|---|
| Adipoq | **-12.28** | Csf1 | -1.46 | Il12a | **-2.22** | Il7 | **-2.71** |
| Bmp2 | **-3.25** | Csf2 | **-10.32** | Il12b | **-6.47** | Il9 | **-8.33** |
| Bmp4 | **-2.79** | Csf3 | **-7.00** | Il13 | **-6.47** | Lif | **-11.55** |
| Bmp6 | **-3.48** | Ctf1 | **-9.75** | Il15 | **-2.24** | Lta | **-4.58** |
| Bmp7 | **-6.54** | Cx3cl1 | **-11.29** | Il16 | 1.15 | Ltb | 1.67 |
| Ccl1 | **-8.15** | Cxcl1 | **-8.50** | Il17a | **-9.80** | Mif | -1.06 |
| Ccl11 | **-6.94** | Cxcl10 | -1.40 | Il17f | -1.77 | Mstn | **-9.32** |
| Ccl12 | **-8.42** | Cxcl11 | **-6.83** | Il18 | 1.19 | Nodal | **-12.48** |
| Ccl17 | **-5.40** | Cxcl12 | 1.54 | Il1a | **-2.36** | Osm | **-3.72** |
| Ccl19 | 1.31 | Cxcl13 | 1.66 | Il1b | -1.51 | Pf4 | 1.27 |
| Ccl2 | **-5.86** | Cxcl16 | -1.63 | Il1rn | **-3.65** | Ppbp | **2.38** |
| Ccl20 | **-9.42** | Cxcl3 | **-8.32** | Il2 | **-7.02** | Spp1 | **-7.16** |
| Ccl22 | **-6.95** | Cxcl5 | **-5.15** | Il21 | **-7.15** | Tgfb2 | **-7.39** |
| Ccl24 | **-13.45** | Cxcl9 | **-4.93** | Il22 | **-6.56** | Thpo | **-7.50** |
| Ccl3 | **-4.77** | Fasl | **-4.92** | Il23a | **-8.75** | Tnf | **-6.47** |
| Ccl4 | **-5.73** | Gpi1 | 1.09 | Il24 | **-8.41** | Tnfrsf11b | **-7.34** |
| Ccl5 | 1.52 | Hc | **-6.84** | Il27 | **-9.03** | Tnfsf10 | **-6.77** |
| Ccl7 | **-7.97** | Ifna2 | **-9.44** | Il3 | **-11.33** | Tnfsf11 | **-10.52** |
| Cd40lg | -1.98 | Ifng | **-5.90** | Il4 | **-6.37** | Tnfsf13b | **-4.10** |
| Cd70 | **-7.65** | Il10 | **-5.82** | Il5 | **-12.05** | Vegfa | -1.75 |
| Cntf | **-2.18** | Il11 | **-9.34** | Il6 | **-10.04** | Xcl1 | **-2.88** |

NOTE. Fold regulation means fold changes of the H2R agonist group compared with the PBS control group. Boldface indicates fold-changes large than 2.

survival, in part through preventing MB-HSC exhaustion (Figure 9).

## Experimental Model and Mice Details

C57BL/6 background HDC-GFP, HDC-/-; HDC-GFP, HDCGFP; HDCCreERT; iDTR mice have been described previously.[1,14] HDC-GFP transgenic mice were generated previously from HDC-enhanced green fluorescent protein (EGFP) bacterial artificial chromosome (BAC) transgenic mice in which EGFP expression was controlled by the murine HDC promoter.[1] HDC-GFP transgenic mice were crossed to previously reported HDC−/− mice[58] in which exon 5 of the HDC gene was replaced with a neomycin cassette. The HDC-CreERT transgenic line was generated by using BAC recombineering from clone RP23-474H6. Founders were backcrossed to C57BL/6 mice for at least 6 generations.[1,14] HDC-CreERT was mated to Rosa26-loxp-stop-loxp-iDTR (iDTR) and HDC-GFP mice to generate HDC-GFP; HDC-CreERT; iDTR mice. The HDC-BAC-GFP transgenic mouse contains several transgene copies of a BAC transgene integrated randomly at a single (non-HDC) chromosomal site, and thus could be bred into an HDC-deficient background yielding HDC−/−; HDC-GFP mice. C57BL/6 WT mice were purchased from the Jackson Laboratory (Bar Harbor, ME). Only 8- to 10-week-old male mice were used in these studies.

Mice were observed carefully by laboratory staff and veterinarian personnel for health and activity. Mice were

**Figure 8.** (***See previous page***). **The role of H2R agonist on myeloid cells in DSS-induced acute colitis.** (*A*) Comparison of the percentage of GFP+ CD11b+Gr1+ cells among CD45+ cells and the (*B*) total number of GFP+CD11b+Gr1+ cells in the BM between the H2R agonist–treated and the PBS group at different time points. (*C*) Comparison of the percentage of GFP+ CD11b+Gr1+ cells among CD45+ cells and the (*D*) total number of GFP+CD11b+Gr1+ cells in the spleen between the H2R agonist–treated and the PBS group at different time points. (*E*) Comparison of the percentage of GFP+CD11b+Gr1+ cells among CD45+ cells and (*F*) among total CD11b+Gr1+ cells in the blood between the H2R agonist–treated and the PBS group at different time points. (*G*) Comparison of the percentage of GFP+CD11b+Gr1+ cells among CD45+ cells and among (*H*) total CD11b+Gr1+ cells in the colon between the H2R agonist–treated and the PBS group at different time points. (*I*) Immunofluorescent images showing GFP+Gr1+ cells in the colon and the (*J*) qualification analysis of GFP+Gr1+ cells of the H2R agonist–treated group and the PBS group. (*K*) Analysis of body weight change and (*L*) Kaplan–Meier curve depicting survival rates of the H2R agonist–treated group and the PBS group. Expression of (*M*) IL6 mRNA and (*N*) csf2 mRNA in the spleen from H2R agonist–treated mice were detected by qRT-PCR. (*O*) Strategy of FACS to analyze the subset of myeloid cells in the spleen. (*P*) Pie charts and (*Q*) histograms for the comparison of the percentage of granulocyte, monocyte, dendritic cell (DC), and macrophage in the spleen between the H2R agonist–treated and the PBS group. Data are expressed as means ± SEM. Results are representative of at least 3 independent experiments. $^{*}P < .05$, $^{**}P < .01$. DAPI, 4′,6-diamidino-2-phenylindole.

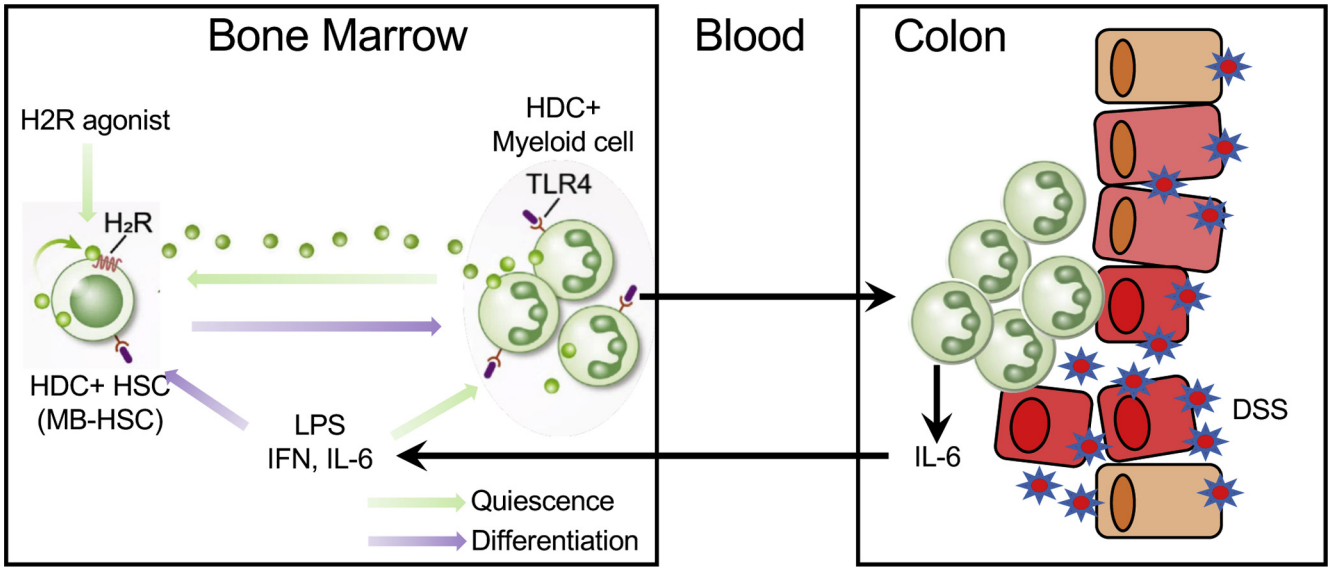


**Figure 9. Schematic of the role of MB-HSCs on acute colitis.** Acute DSS-induced colitis initiates the recruitment of HDC+ myeloid cells from the bone marrow and a loss of quiescence by bone marrow HDC+ MB-HSCs, leading to enhanced myeloid cell production and eventual bone marrow HSC exhaustion. The loss of HDC expression resulted in more rapid MB-HSC activation and depletion, with worse outcomes. Treatment with the H2R agonist dimaprit significantly enhanced survival by preventing MB-HSC exhaustion.

monitored to ensure that food and fluid intake met their nutritional needs. Body weights were recorded at a minimum of weekly, and more often for animals requiring greater attention. Mice were maintained on wood chip bedding, given ad libitum access to water and standard mouse chow, with 12-hour light-dark phase cycles. The colonies were specific pathogen free and tested quarterly for known pathogens. Mice in the barrier facilities were housed in cages with microisolator tops on ventilated or static racks. All caging materials and bedding were autoclaved. Food was irradiated and water was either reverse osmosis, autoclaved, or acidified, depending on the barrier. All manipulations were performed in laminar flow hoods. All mouse studies were approved by the Columbia University Institutional Animal Care and Use Committee.

## Materials and Methods

### *Animal Models*

In acute colitis experiments, HDC-GFP and HDC-/-; HDC-GFP mice were treated with 5% DSS in drinking water. In BrdU incorporation experiments, 1 mg BrdU (BD Biosciences, San Jose, CA) per 6 g body weight was injected intraperitoneally to either HDC-GFP or HDC-/-; HDC-GFP mice. BrdU incorporation was detected 14 hours after injection by using the BD Biosciences BrdU flow kit. For myeloid-depletion experiments, 250 ng DT (List Biological Labs, Campbell, CA) was injected intraperitoneally every other day for 4 days after DSS initiation, and tamoxifen chow (Harlan Laboratories, Itingen, BL) regimen was applied 4 days before DSS initiation to deplete HDC+ myeloid cells in HDC-GFP; HDC- CreERT2; iDTR mice. For DSS-induced intestine injury protection experiments, the H2R agonist dimaprit dihydrochloride (100 ug/mouse; Tocris Bioscience, Minneapolis, MN) or PBS was injected intraperitoneally twice a day, and TLR4 antagonist (E5564, 5 mg/kg body weight; Eisai, Inc, Woodcliff Lake, NJ) was injected into the tail vain once a day for 7 consecutive days after DSS initiation.

### *Flow Cytometry Analysis*

Mouse bones were flushed or crushed using a mortar and pestle with Ca2+ and Mg2+ free Hank's balanced salt solution supplemented with 2% heat-inactivated fetal bovine serum. A single-cell suspension from spleen was obtained by mashing the tissue with a syringe plunger end against a cell strainer. Blood was collected in EDTA-containing tubes (BD Diagnostics, Franklin Lakes, NJ) by puncturing the submandibular vein. Red blood cells, splenic cells, and bone marrow cells were lysed (red blood cell lysis buffer, BioLegend, San Diego, CA) before passing through a 70-mm nylon mesh. Hematopoietic stem and progenitor cells were defined by immunophenotype, as follows: HSPC: Lin-c-kit+Sca-1+ (LSK); HSC: LSKCD150+CD48-; and myeloid cell: CD11b+Gr1+. The following antibodies were used: CD150 (TC15-12F12.2), CD48 (HM48-1), c-kit (2B8), Sca-1 (E13-161.7), and CD16/32 (FcgR, 93). Lineage cells were stained using CD2 (RM2-5), CD3 (17A2), CD5 (53-7.3), CD8a (53-6.7), TER-119 (TER-119), B220 (RA3-6B2), and Gr1 (RB6- 8C5). Other antibodies used in this study include CD11b (M1/70), CD45 (30-F11), CD11c (3.9), Ly6G (1A8), Ly6C (HK1.4), and F4/80 (BM8). For cell-cycle analysis, bone marrow cells first were stained with cell surface markers, then fixed and permeabilized (BD cytofix/cytoperm solutions, BD Biosciences), followed by staining with anti-Ki67 (16A8) and Hoechst 33342 (BD PharMingen, San Jose, CA). For BrdU incorporation experiments, HDC-GFP+

and HDC-GFP- cells were separated and analyzed using BD PharMingen BrdU Flow Kits according to the manufacturer's instructions. All FACS analyses were performed on LSRII instrument (BD Biosciences).

### Immunofluorescence Microscopy and Histopathology

Dissected mouse colon was fixed in 4% paraformaldehyde, embedded in optimal cutting temperature, and snap-frozen in liquid nitrogen. Slides were permeabilized with 0.05% Triton X-100 (Thermo Fisher Scientific, Waltham, MA) in PBS and blocked with 5% normal goat serum. Primary antibodies (anti-GFP, 1:200, Abcam, Cambridge, UK; anti-Gr1, 1:200, BioLegend) were applied for overnight staining. Alexa Fluor secondary antibodies (Invitrogen, Waltham, MA) were used to show staining. All slides were counterstained and mounted with ProLong antifade mounting medium (Invitrogen). Fluorescence images were acquired with an A1 laser scanning confocal attachment on an Eclipse Ti microscope stand (Nikon Instruments, Melville, NY).

To show the tissue histopathology and evaluate the severity of the histologic scoring system, H&E staining was performed on formalin-fixed, paraffin-embedded tissue. The severities of DSS-induced acute colitis were graded according to previous studies.[59,60] The histologic score was calculated by the sum of inflammation severity (0, none; 1, mild; 2, moderate; and 3, severe), inflammation extent (0, none; 1, mucosa; 2, submucosa; and 3, transmural), crypt damage (0, none; 1, basal 1/3 damage; 2, basal 2/3 damage; 3, crypt lost, surface epithelium present; and 4, crypt and surface epithelium lost), and the percentage of tissue involved (0, 0%; 1, 1%–25%; 2, 26%–50%; 3, 51%–75%; and 4, 76%–100%). The total score was a maximum of 14.

### Cytokine and Chemokine qRT-PCR Array and qRT-PCR

Total RNA from spleen tissue was exacted by the RNeasy Micro kit (QIAGEN, Hiden, Germany) following the manufacturer's instructions. Complementary DNA was synthesized with a mixture of random and Oligo deoxythymidine (dT) primers using SuperScript III Reverse Transcriptase (Life Technologies, Carlsbad, CA).

Detection and quantification of gene expression were performed using a Mouse Cytokines and Chemokines RT2 Profiler PCR Array (PAMM-150Z; QIAGEN) and FastStart Universal SYBR Green Master (Rox) (Roche Molecular Systems, Pleasanton, CA) according to the manufacturer's instructions. The cycle -threshold (CT) data were uploaded into the data analysis template on the manufacturer's website (https://geneglobe.qiagen.com/jp/analyze). The RNA expression of each gene was normalized using 5 housekeeping genes as controls. The relative expression of each gene, compared with the expression in the control group, was calculated on the website using the ΔΔCT method. A difference was considered significant at $P < .05$. In the expression studies, a gene was considered differentially regulated if the difference was more than 2-fold compared with the control.

The primer sequences of SYBR Green qRT-PCR assays are as follows: IL6 (forward: 5'-AAACCGCTATGAAGTTCCTCTC-3'; reverse: 5'-GTGGTATCCTCTGTGAAGTCTC-3'), Csf2 (forward: 5'-AGAGGCCATCAAAGAAGCCC-3'; reverse: 5'-AAATTGCCCCGTAGACCCTG-3'), and glyceraldehyde-3-phosphate dehydrogenase (forward: 5'-CTTTGTCAAGCTCATTTCCTGG-3'; reverse: 5'-TCTTGCTCAGTGTCCTTGC-3'). qPCR was performed with the Applied Biosystems Prism 9700 PCR machine (Foster City, CA). Relative gene expression was normalized to glyceraldehyde-3-phosphate dehydrogenase.

### Statistical Analysis

Statistical analysis was performed to detect the significance of differences in the means of the abundance of mRNA or cell types, or of survival, in the different conditions being compared. All data are shown as the means ± SEM. Kaplan–Meier survival was statistically analyzed by the log-rank test. Other statistical comparisons were evaluated with the Student $t$ test or 1-way analysis of variance. Statistical analysis was performed using Prism 8 (GraphPad, San Diego, CA). For each experiment the specific statistical details can be found in the figure legends.

## References


1. Yang XD, Ai W, Asfaha S, Bhagat G, Friedman RA, Jin G, Park H, Shykind B, Diacovo TG, Falus A, Wang TC. Histamine deficiency promotes inflammation-associated carcinogenesis through reduced myeloid maturation and accumulation of CD11b+Ly6G+ immature myeloid cells. Nat Med 2011;17:87–95.
2. Takeda K, Akira S. Toll-like receptors. Curr Protoc Immunol 2015;109:14.2.1–.2.0.
3. Malvin NP, Seno H, Stappenbeck TS. Colonic epithelial response to injury requires Myd88 signaling in myeloid cells. Mucosal Immunol 2012;5:194–206.
4. Wynn TA, Vannella KM. Macrophages in tissue repair, regeneration, and fibrosis. Immunity 2016;44:450–462.
5. Pull SL, Doherty JM, Mills JC, Gordon JI, Stappenbeck TS. Activated macrophages are an adaptive element of the colonic epithelial progenitor niche necessary for regenerative responses to injury. Proc Natl Acad Sci U S A 2005;102:99–104.
6. Ghia JE, Galeazzi F, Ford DC, Hogaboam CM, Vallance BA, Collins S. Role of M-CSF-dependent macrophages in colitis is driven by the nature of the inflammatory stimulus. Am J Physiol Gastrointest Liver Physiol 2008;294:G770–G777.
7. King KY, Goodell MA. Inflammatory modulation of HSCs: viewing the HSC as a foundation for the immune response. Nat Rev Immunol 2011;11:685–692.
8. Rodriguez S, Chora A, Goumnerov B, Mumaw C, Goebel WS, Fernandez L, Baydoun H, HogenEsch H, Dombkowski DM, Karlewicz CA, Rice S, Rahme LG, Carlesso N. Dysfunctional expansion of hematopoietic

stem cells and block of myeloid differentiation in lethal sepsis. Blood 2009;114:4064–4076.
9. Manz MG, Boettcher S. Emergency granulopoiesis. Nat Rev Immunol 2014;14:302–314.
10. Ema H, Morita Y, Suda T. Heterogeneity and hierarchy of hematopoietic stem cells. Exp Hematol 2014;42:74–82.e2.
11. Land RH, Rayne AK, Vanderbeck AN, Barlowe TS, Manjunath S, Gross M, Eiger S, Klein PS, Cunningham NR, Huang J, Emerson SG, Punt JA. The orphan nuclear receptor NR4A1 specifies a distinct subpopulation of quiescent myeloid-biased long-term HSCs. Stem Cells 2015;33:278–288.
12. Morita Y, Ema H, Nakauchi H. Heterogeneity and hierarchy within the most primitive hematopoietic stem cell compartment. J Exp Med 2010; 207:1173–1182.
13. Walter D, Lier A, Geiselhart A, Thalheimer FB, Huntscha S, Sobotta MC, Moehrle B, Brocks D, Bayindir I, Kaschutnig P, Muedder K, Klein C, Jauch A, Schroeder T, Geiger H, Dick TP, Holland-Letz T, Schmezer P, Lane SW, Rieger MA, Essers MA, Williams DA, Trumpp A, Milsom MD. Exit from dormancy provokes DNA-damage-induced attrition in haematopoietic stem cells. Nature 2015;520:549–552.
14. Chen X, Deng H, Churchill MJ, Luchsinger LL, Du X, Chu TH, Friedman RA, Middelhoff M, Ding H, Tailor YH, Wang ALE, Liu H, Niu Z, Wang H, Jiang Z, Renders S, Ho SH, Shah SV, Tishchenko P, Chang W, Swayne TC, Munteanu L, Califano A, Takahashi R, Nagar KK, Renz BW, Worthley DL, Westphalen CB, Hayakawa Y, Asfaha S, Borot F, Lin CS, Snoeck HW, Mukherjee S, Wang TC. Bone marrow myeloid cells regulate myeloid-biased hematopoietic stem cells via a histamine-dependent feedback loop. Cell Stem Cell 2017; 21:747–760.e7.
15. Ai W, Takaishi S, Wang TC, Fleming JV. Regulation of L-histidine decarboxylase and its role in carcinogenesis. Prog Nucleic Acid Res Mol Biol 2006;81:231–270.
16. van der Pouw Kraan TC, Snijders A, Boeije LC, de Groot ER, Alewijnse AE, Leurs R, Aarden LA. Histamine inhibits the production of interleukin-12 through interaction with H2 receptors. J Clin Invest 1998; 102:1866–1873.
17. Elenkov IJ, Webster E, Papanicolaou DA, Fleisher TA, Chrousos GP, Wilder RL. Histamine potently suppresses human IL-12 and stimulates IL-10 production via H2 receptors. J Immunol 1998;161:2586–2593.
18. Hirasawa N, Shiraishi M, Tokuhara N, Hirano Y, Mizutani A, Mue S, Ohuchi K. Pharmacological analysis of the inflammatory exudate-induced histamine production in bone marrow cells. Immunopharmacology 1997; 36:87–94.
19. Paquay JB, Hoen PA, Voss HP, Bast A, Timmerman H, Haenen GR. Nitric oxide synthase inhibition by dimaprit and dimaprit analogues. Br J Pharmacol 1999; 127:331–334.
20. Motoki A, Adachi N, Liu K, Takahashi HK, Nishibori M, Yorozuya T, Arai T, Nagaro T. Suppression of ischaemia-induced cytokine release by dimaprit and amelioration of liver injury in rats. Basic Clin Pharmacol Toxicol 2008; 102:394–398.
21. Nakamura T, Ueno Y, Goda Y, Nakamura A, Shinjo K, Nagahisa A. Efficacy of a selective histamine H2 receptor agonist, dimaprit, in experimental models of endotoxin shock and hepatitis in mice. Eur J Pharmacol 1997; 322:83–89.
22. Fray A, Burtin C, Scheinmann P, Lespinats G, Canu P. In vivo and in vitro anti-tumour activity of dimaprit. Agents Actions 1985;16:284–286.
23. Eichele DD, Kharbanda KK. Dextran sodium sulfate colitis murine model: an indispensable tool for advancing our understanding of inflammatory bowel diseases pathogenesis. World J Gastroenterol 2017; 23:6016–6029.
24. Kiesler P, Fuss IJ, Strober W. Experimental models of inflammatory bowel diseases. Cell Mol Gastroenterol Hepatol 2015;1:154–170.
25. Vicario M, Crespí M, Franch A, Amat C, Pelegrí C, Moretó M. Induction of colitis in young rats by dextran sulfate sodium. Dig Dis Sci 2005;50:143–150.
26. Zeeff SB, Kunne C, Bouma G, de Vries RB, Te Velde AA. Actual usage and quality of experimental colitis models in preclinical efficacy testing: a scoping review. Inflamm Bowel Dis 2016;22:1296–1305.
27. Munyaka PM, Rabbi MF, Khafipour E, Ghia JE. Acute dextran sulfate sodium (DSS)-induced colitis promotes gut microbial dysbiosis in mice. J Basic Microbiol 2016; 56:986–998.
28. Mullarkey M, Rose JR, Bristol J, Kawata T, Kimura A, Kobayashi S, Przetak M, Chow J, Gusovsky F, Christ WJ, Rossignol DP. Inhibition of endotoxin response by e5564, a novel Toll-like receptor 4-directed endotoxin antagonist. J Pharmacol Exp Ther 2003; 304:1093–1102.
29. Ayres JS, Trinidad NJ, Vance RE. Lethal inflammasome activation by a multidrug-resistant pathobiont upon antibiotic disruption of the microbiota. Nat Med 2012; 18:799–806.
30. Saha S, Aranda E, Hayakawa Y, Bhanja P, Atay S, Brodin NP, Li J, Asfaha S, Liu L, Tailor Y, Zhang J, Godwin AK, Tome WA, Wang TC, Guha C, Pollard JW. Macrophage-derived extracellular vesicle-packaged WNTs rescue intestinal stem cells and enhance survival after radiation injury. Nat Commun 2016;7:13096.
31. Perše M, Cerar A. Dextran sodium sulphate colitis mouse model: traps and tricks. J Biomed Biotechnol 2012; 2012:718617.
32. Schuettpelz LG, Link DC. Regulation of hematopoietic stem cell activity by inflammation. Front Immunol 2013; 4:204.
33. Drakos PE, Nagler A, Or R. Case of Crohn's disease in bone marrow transplantation. Am J Hematol 1993; 43:157–158.

34. Griseri T, McKenzie BS, Schiering C, Powrie F. Dysregulated hematopoietic stem and progenitor cell activity promotes interleukin-23-driven chronic intestinal inflammation. Immunity 2012;37:1116–1129.
35. Coppin E, Florentin J, Vasamsetti SB, Arunkumar A, Sembrat J, Rojas M, Dutta P. Splenic hematopoietic stem cells display a pre-activated phenotype. Immunol Cell Biol 2018. https://doi.org/10.1111/imcb.12035.
36. Morita Y, Iseki A, Okamura S, Suzuki S, Nakauchi H, Ema H. Functional characterization of hematopoietic stem cells in the spleen. Exp Hematol 2011;39:351–359.e3.
37. Zhou J, Lai W, Yang W, Pan J, Shen H, Cai Y, Yang C, Ma N, Zhang Y, Zhang R, Xie X, Dong Z, Gao Y, Du C. BLT1 in dendritic cells promotes Th1/Th17 differentiation and its deficiency ameliorates TNBS-induced colitis. Cell Mol Immunol 2018;15:1047–1056.
38. Wirtz S, Popp V, Kindermann M, Gerlach K, Weigmann B, Fichtner-Feigl S, Neurath MF. Chemically induced mouse models of acute and chronic intestinal inflammation. Nat Protoc 2017;12:1295–1309.
39. Hernandez-Chirlaque C, Aranda CJ, Ocon B, Capitan-Canadas F, Ortega-Gonzalez M, Carrero JJ, Suarez MD, Zarzuelo A, Sanchez de Medina F, Martinez-Augustin O. Germ-free and antibiotic-treated mice are highly susceptible to epithelial injury in DSS colitis. J Crohns Colitis 2016;10:1324–1335.
40. DeVoss J, Diehl L. Murine models of inflammatory bowel disease (IBD): challenges of modeling human disease. Toxicol Pathol 2014;42:99–110.
41. Morris GP, Beck PL, Herridge MS, Depew WT, Szewczuk MR, Wallace JL. Hapten-induced model of chronic inflammation and ulceration in the rat colon. Gastroenterology 1989;96:795–803.
42. Kuhn R, Lohler J, Rennick D, Rajewsky K, Muller W. Interleukin-10-deficient mice develop chronic enterocolitis. Cell 1993;75:263–274.
43. Qin Y, Zhang C. The regulatory role of IFN-$\gamma$ on the proliferation and differentiation of hematopoietic stem and progenitor cells. Stem Cell Rev Rep 2017;13:705–712.
44. Rezzoug F, Huang Y, Tanner MK, Wysoczynski M, Schanie CL, Chilton PM, Ratajczak MZ, Fugier-Vivier IJ, Ildstad ST. TNF-alpha is critical to facilitate hemopoietic stem cell engraftment and function. J Immunol 2008;180:49–57.
45. Zhang H, Rodriguez S, Wang L, Wang S, Serezani H, Kapur R, Cardoso AA, Carlesso N. Sepsis induces hematopoietic stem cell exhaustion and myelosuppression through distinct contributions of TRIF and MYD88. Stem Cell Rep 2016;6:940–956.
46. Baldridge MT, King KY, Boles NC, Weksberg DC, Goodell MA. Quiescent haematopoietic stem cells are activated by IFN-gamma in response to chronic infection. Nature 2010;465:793–797.
47. Nagai Y, Garrett KP, Ohta S, Bahrun U, Kouro T, Akira S, Takatsu K, Kincade PW. Toll-like receptors on hematopoietic progenitor cells stimulate innate immune system replenishment. Immunity 2006;24:801–812.
48. Parsons ME, Owen DA, Ganellin CR, Durant GJ. Dimaprit -(S-[3-(N,N-dimethylamino)prophyl]isothiourea) - a highly specific histamine H2 -receptor agonist. Part 1. Pharmacology. Agents Actions 1977;7:31–37.
49. Neumann D, Seifert R. The therapeutic potential of histamine receptor ligands in inflammatory bowel disease. Biochem Pharmacol 2014;91:12–17.
50. Wechsler JB, Szabo A, Hsu CL, Krier-Burris RA, Schroeder HA, Wang MY, Carter RG, Velez TE, Aguiniga LM, Brown JB, Miller ML, Wershil BK, Barrett TA, Bryce PJ. Histamine drives severity of innate inflammation via histamine 4 receptor in murine experimental colitis. Mucosal Immunol 2018;11:861–870.
51. Hunter CA, Jones SA. IL-6 as a keystone cytokine in health and disease. Nat Immunol 2015;16:448–457.
52. Murakami M, Kamimura D, Hirano T. Pleiotropy and specificity: insights from the interleukin 6 family of cytokines. Immunity 2019;50:812–831.
53. Tie R, Li H, Cai S, Liang Z, Shan W, Wang B, Tan Y, Zheng W, Huang H. Interleukin-6 signaling regulates hematopoietic stem cell emergence. Exp Mol Med 2019;51:1–12.
54. Kondo M, Wagers AJ, Manz MG, Prohaska SS, Scherer DC, Beilhack GF, Shizuru JA, Weissman IL. Biology of hematopoietic stem cells and progenitors: implications for clinical application. Annu Rev Immunol 2003;21:759–806.
55. Kimura A, Rieger MA, Simone JM, Chen W, Wickre MC, Zhu BM, Hoppe PS, O'Shea JJ, Schroeder T, Hennighausen L. The transcription factors STAT5A/B regulate GM-CSF-mediated granulopoiesis. Blood 2009;114:4721–4728.
56. Bailly S, Ferrua B, Fay M, Gougerot-Pocidalo MA. Differential regulation of IL 6, IL 1 A, IL 1 beta and TNF alpha production in LPS-stimulated human monocytes: role of cyclic AMP. Cytokine 1990;2:205–210.
57. Bauer J, Ganter U, Geiger T, Jacobshagen U, Hirano T, Matsuda T, Kishimoto T, Andus T, Acs G, Gerok W, et al. Regulation of interleukin-6 expression in cultured human blood monocytes and monocyte-derived macrophages. Blood 1988;72:1134–1140.
58. Ohtsu H, Tanaka S, Terui T, Hori Y, Makabe-Kobayashi Y, Pejler G, Tchougounova E, Hellman L, Gertsenstein M, Hirasawa N, Sakurai E, Buzas E, Kovacs P, Csaba G, Kittel A, Okada M, Hara M, Mar L, Numayama-Tsuruta K, Ishigaki-Suzuki S, Ohuchi K, Ichikawa A, Falus A, Watanabe T, Nagy A. Mice lacking histidine decarboxylase exhibit abnormal mast cells. FEBS Lett 2001;502:53–56.

59. Kihara N, de la Fuente SG, Fujino K, Takahashi T, Pappas TN, Mantyh CR. Vanilloid receptor-1 containing primary sensory neurones mediate dextran sulphate sodium induced colitis in rats. Gut 2003;52:713–719.
60. Yu Y, Song EM, Lee KE, Joo YH, Kim SE, Moon CM, Kim HY, Jung SA, Jo I. Therapeutic potential of tonsil-derived mesenchymal stem cells in dextran sulfate sodium-induced experimental murine colitis. PLoS One 2017;12:e0183141.

**Received August 20, 2020. Accepted November 10, 2020.**

**Correspondence**
Address correspondence to: Timothy C. Wang, MD, Division of Digestive and Liver Diseases, Department of Medicine, Columbia University Medical Center, Irving Cancer Research Center, 1130 St. Nicholas Avenue, New York, New York, 10032. e-mail: tcw21@cumc.columbia.edu; fax: (212) 851-4590.

**Acknowledgments**
The authors thank the Columbia Center for Translational Immunology (CCTI) Flow Cytometry Core (supported in part by the Office of the Director, National Institutes of Health, awards S10OD020056 and S10RR027050) for FACS analysis.

**CRediT Authorship Contributions**
Na Fu (Conceptualization: Lead; Writing – original draft: Lead);
Feijing Wu (Software: Supporting); Zhengyu Jiang (Software: Supporting);
Woosook Kim (Software: Supporting); Tuo Ruan (Software: Supporting);
Ermanno Malagola (Formal analysis: Supporting)
Yosuke Ochiai (Formal analysis: Supporting);
Osmel Companioni Nápoles (Formal analysis: Equal);
Giovanni Valenti (Formal analysis: Supporting);
Ruth A. White (Methodology: Supporting); Bryana R. Belin (Project administration: Supporting);
Leah B. Zamechek (Project administration: Supporting);
Jonathan S. LaBella (Project administration: Supporting);
Timothy Cragin Wang, MD (Funding acquisition: Supporting; Supervision: Lead; Writing – review & editing: Lead).

**Conflicts of interest**
The authors disclose no conflicts.

**Funding**
This work was supported by National Institute of Diabetes and Digestive and Kidney Disorders of the National Institutes of Health grant 5R01DK048077-23 (T.C.W.). The content is solely the responsibility of the authors and does not necessarily represent the official views of the National Institutes of Health.